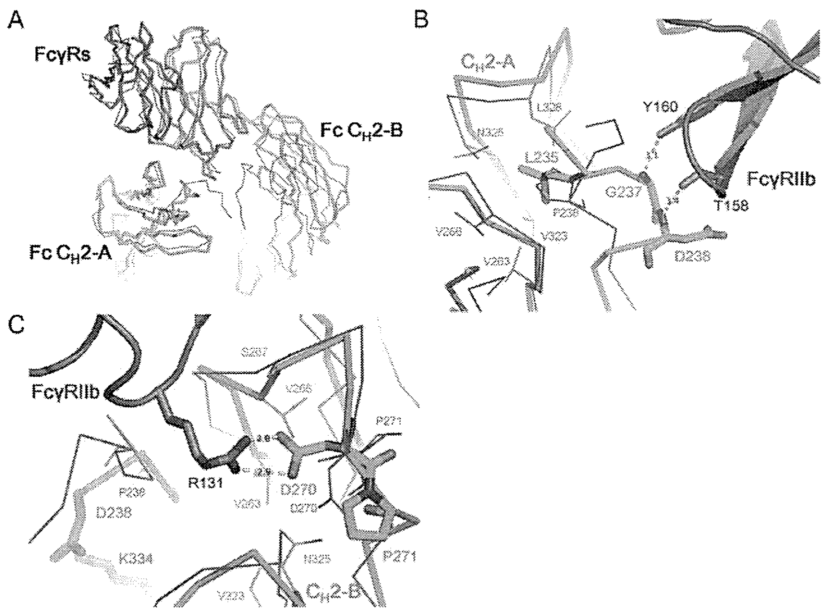

Fig. 3. Structural comparison of Fc(P238D)/FcγRIIb complex with Fc(IgG1)/FcγRIIa^{R131} complex. (**A**) The overall structural comparison of Fc(P238D)/FcγRIIb complex with Fc(IgG1)/FcγRIIa^{R131} complex. (**B**) The binding interface between the C_H2-A domain of Fc(P238D) and FcγRIIb. (**C**) The binding interface between the C_H2-B domain and FcγRIIb. The structural changes and novel interactions introduced by P238D in both interfaces are shown by comparing Fc(P238D)/FcγRIIb and Fc(IgG1)/ FcγRIIa^{R131}. Fc(P238D)/FcγRIIb and Fc(IgG1)/FcγRIIa^{R131} are shown in green and magenta, respectively. FcγRIIb and FcγRIIa^{R131} are shown in the darker color, respectively.

Table I. Effect of additional substitution(s) into P238D variant on binding affinity for FcγRIIb

Variant no.	Amino acid change					Fold (K_D for FcγRIIb)
Single substitution						
V1	E233D					1.7
V2		G237D				1.5
V3			H268D			1.7
V4				P271G		5.0
V5					A330R	1.2
Two substitutions						
V6	E233D				A330R	1.9
Three substitutions						
V7	E233D			P271G	A330R	8.2
V8		G237D	H268D	P271G		9.5
V9		G237D		P271G	A330R	33
Four substitutions						
V10	E233D		H268D	P271G	A330R	9.0
V11		G237D	H268D	P271G	A330R	40
Five substitutions						
V12	E233D	G237D	H268D	P271G	A330R	62

Fold = K_D (P238D variant)/K_D (Fc variants).

Screening, characterization and design of variants to further enhance FcγRIIb binding by comprehensive mutagenesis using the P238D variant as a template

In order to further enhance the affinity to FcγRIIb, we combined P238D with L328E or S267E/L328F, previously known variant to increase binding to FcγRIIb and FcγRIIa^{R131}. Unexpectedly, the additive effect by combining P238D with those substitutions was not observed. Affinities for FcγRIIb of these variants are listed in Supplementary Table S3.

Then, we screened substitutions to improve FcγRIIb binding when they were combined with P238D by comprehensive mutagenesis using the P238D variant as a template. Approximately 400 variants with an additional single substitution onto the P238D variant were generated, and the affinity for FcγRIIb was determined. Six effective substitutions (E233D, G237D, H268D, P271G, Y296D and A330R) were identified. We further combined these substitutions to create V12 variant having all the six substitutions described above. The fold increases of the variants against FcγRIIb over P238D variant are listed in Table I.

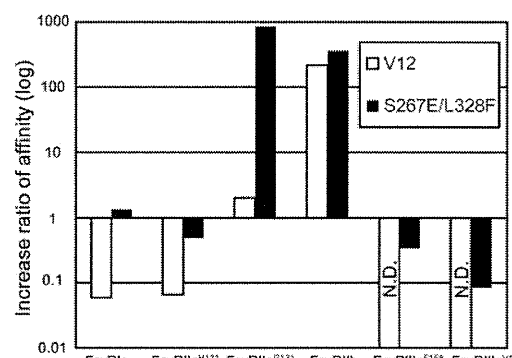

Fig. 4. Affinity ratio of S267E/L328F and V12 variant for all the human FcγRs. The binding of V12 variant to FcγRIIIa^{F158} or FcγRIIIa^{V158} was not detected. Affinity ratio was calculated by the equation, K_D (IgG1)/K_D (Fc variant).

K_Ds of wild-type IgG1, S267E/L328F variant and the most potent variant, V12 variant, to all the FcγRs are listed in Supplementary Table S2 and the changes in affinity from IgG1 are shown in Fig. 4. V12 variant showed 217-fold increase in affinity for FcγRIIb, yet bound to FcγRIIa^{R131} with similar affinity to that of wild-type IgG1 and to the other activating FcγRs with affinity significantly lower than that of IgG1. On the other hand, S267E/L328F variant increased the affinity for FcγRIIb 355-fold and that for FcγRIIa^{R131} even greater, 864-fold.

Crystal structure of the FcγRIIb complex with Fc(V12)

The same conformational changes around Asp238 induced by P238D substitution in Fc(P238D)/FcγRIIb were also observed in Fc(V12)/FcγRIIb.

In the C_H2-A domain, the introduced residues, Asp233, Asp237 and Arg330, were located in the interface with FcγRIIb (Fig. 5A). The weak electron density of Asp233, replaced from Glu, was observed. As Lys113 of FcγRIIb is located near Asp233, they might interact with each other. In the C_H2-A domain, Asp237, replaced from Gly, made van der Waals contacts with Trp87 and Tyr160 of FcγRIIb. In addition, the hydrogen bond distance between NH of the main chain at position 237 in Fc and OH of the Tyr160 side chain in FcγRIIb changed from 3.1 Å in Fc(P238D) (Fig. 3C) to 2.9 Å in Fc(V12) (Fig. 5A). A weak hydrogen bond between the side chain of Asp238 and the side chain of Thr158 of FcγRIIb was also observed. The electron density of the side chain of Arg330, which replaced Ala, was not clearly observed. As Glu86 of FcγRIIb is located near Arg330, a weak interaction between those residues could be present.

In the C_H2-B domain, H268D and P271G substitutions induced a further conformational change of a loop around Asp270 (Fig. 5B). The substitution from Pro to Gly at position 271 caused the main chain to flip and consequently rearranged the 266–273 loop and Arg131 of FcγRIIb, which also formed a salt bridge with Asp270 in C_H2-B of Fc(V12) as well as in Fc(P238D). In addition, the electron density of Gly271 in C_H2-B was clearly observed, though in Pro271 in Fc(P238D) it was not. This conformational change of the loop caused a rearrangement of Arg292 in C_H2-B of Fc(V12). The other substituted residue, Asp268, formed an electrostatic interaction with the shifted Arg292.

Pharmacokinetic and biophysical property assessment of V12 variant

In order to characterize the pharmacokinetic aspect of V12 variant, we measured the affinity for hFcRn and the pharmacokinetics in hFcRn transgenic mice. The binding affinity of V12 variant for hFcRn at pH6.0 was comparable with that of wild-type IgG1 and the *in vivo* half-life was also comparable (Table II).

T_M of the C_H2 domain was measured by thermal shift assay. The T_M of V12 variant decreased by 8°C relative to wild-type IgG1 (Table II). To assess the real-time stability for pharmaceutical application of V12 variant, a stability study at an antibody concentration of 100 mg/ml was performed. The formation of HMW species of V12 variant after storage for 4 weeks at 25°C was comparable with that of wild-type IgG1 (Table II).

In vitro *activation and aggregation of platelets by ICs consisting of IgE and anti-IgE antibody with S267E/L328F variant or V12 variant*

Platelets obtained from two donors homozygous for FcγRIIa^{R131} genotype and incubated with IC consisting of IgE and anti-IgE S267E/L328F variant increased the expression of CD62p and PAC-1 on the platelets, but those incubated with IC consisting of IgE and anti-IgE with the V12 variant did not (Supplementary Fig. S2A and B). On the other hand, when we used platelets obtained from two donors homozygous for FcγRIIa^{H131} genotype, IC consisting of IgE and anti-IgE S267E/L328F variant slightly upregulated the expression of CD62p and PAC-1 on the platelets but IC consisting of anti-IgE with the V12 variant did not after the incubation compared with the control (phosphate-buffered saline) (Supplementary Fig. S2C and D).

Next, the platelet aggregation induced by ICs was evaluated with an aggregometer. After the addition of ADP, only IC consisting of IgE and anti-IgE with S267E/L328F substitutions aggregated the platelets obtained from two donors homozygous for FcγRIIa^{R131} genotype, while IC consisting of IgE and anti-IgE with V12 variant did not (Fig. 6A and B). On the other hand, IC consisting of neither variant induced the aggregation of the platelets obtained from two donors homozygous for FcγRIIa^{H131} genotype (Fig. 6C and D).

Enhancement of agonistic activity of anti-CD137 antibody with enhanced FcγRIIb binding Fc

Several reports have described that agonistic anti-TNFR superfamily antibodies generally require FcγRIIb coengagment for their agonistic activity and that enhancing the binding affinity of the antibodies for FcγRIIb could increase the agonistic activity (White *et al.*, 2011; Wilson *et al.*, 2011; Li and Ravetch, 2012). Therefore, we tested whether V12 also has the same property using agonist antibody against CD137 (clone 1D8), which is one of the TNFR superfamily.

Mouse T lymphoma cell line CTLL-2 was used as mouse CD137-expressing cells (Fig. 7A), and human B lymphoma cell line Raji was used as human FcγRII-positive cells (Hernández *et al.*, 2010). T-cell activating agonistic activity of anti-CD137 antibody was measured with the production of mouse IFN-γ production of CTLL-2 co-cultured with Raji cells. Consistent with the previous reports, V12 variant as well as S267E/L328F variant increased IFN-γ production induced by agonist anti-CD137 antibody compared with intact human IgG1 by more than 5-fold (Fig. 7B).

Discussion

Several efforts to improve FcγR binding by Fc engineering have been reported to date. While most of the engineering enhances the binding affinity for activating FcγRs (Stavenhagen *et al.*, 2007; Zalevsky *et al.*, 2009; Mossner *et al.*, 2010), engineering to enhance binding affinity to inhibitory FcγR is limited (Chu *et al.*, 2008). S267E/L328F variant, the Fc variant reported to have the highest affinity for inhibitory FcγR binding, enhanced the binding affinity for FcγRIIb by 355-fold; however, it also enhanced the binding affinity for FcγRIIa^{R131} to the same level as FcγRIIb (Smith *et al.*, 2012). The high similarity between FcγRIIb and FcγRIIa^{R131} suggests that discriminating FcγRIIb and FcγRIIa^{R131} by Fc engineering is challenging (Supplementary Fig. S1).

In this work, we investigated the substitutions to distinguish FcγRIIb from FcγRIIa^{R131} by comprehensive mutagenesis and discovered a highly selective substitution, P238D, which provides the highest selectivity for FcγRIIb relative to all the other active FcγRs including FcγRIIa^{R131}. Fc variants which discriminate FcγRIIb from FcγRIIa^{R131} were extremely rare, probably because FcγRIIb is highly homologous to

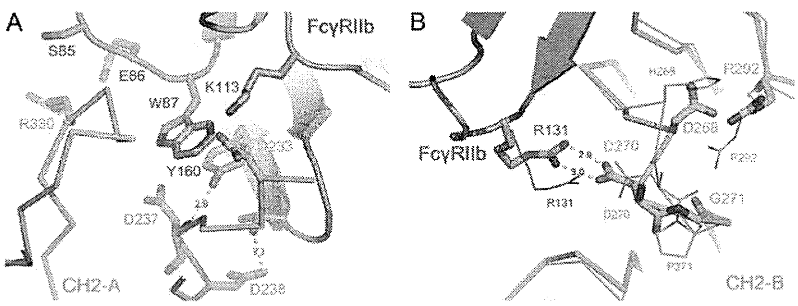

Fig. 5. Structure of Fc(V12)/FcγRIIb complex. (**A**) The binding interface between the C_H2-A domain of Fc(V12) and FcγRIIb. The substitutions in Fc(V12) and the residues in FcγRIIb with a minimum distance of 3.8 Å from these substitutions are shown as sticks. (**B**) The binding interface between the C_H2-B domain of Fc(V12) and FcγRIIb. The structural changes around Asp270 in the C_H2-B domains shown by comparing Fc(P238D)/FcγRIIb (green) and Fc(P238D)/FcγRIIb (cyan) complexes. FcγRIIb in each complex is shown in the darker color.

Table II. Characterization of V12 variant

	T_M (CH2) (°C)	HMW formation after storage (%)	K_D for FcRn (μM)[a]	Half-life (day)[b]
IgG1	70	0.30	1.5 ± 0.0	12.8 ± 3.8
V12	62	0.33	1.4 ± 0.0	12.6 ± 3.2

The group mean ± SD are given for the parameter (n = 3 each).
[a]K_D for FcRn was measured at pH6.0 by SPR.
[b]Half-life of intravenously injected IgG1 and V12 variant at 1 mg/kg in hFcRn transgenic mouse.

FcγRIIa^{R131} (Supplementary Fig. S1) and the Fc-FcγRIIb interface would be also highly homologous to the Fc-FcγRIIa^{R131}. To the best of our knowledge, this is the first report illustrating an Fc variant that enhances FcγRIIb binding while distinguishing FcγRIIb and FcγRIIa^{R131} precisely.

To elucidate the structural mechanism by which P238D variant discriminates FcγRIIb from FcγRIIa^{R131}, we solved the crystal structure of the complex of Fc(P238D) and FcγRIIb. Our structural analysis indicated that the high selectivity of P238D variant was achieved by a dynamic conformational change of the Fc-FcγRIIb interface that was induced by P238D substitution into wild-type IgG1. In reported Fc(IgG1) structures, Pro238 forms a hydrophobic core with its surrounding residues. Therefore, substituting this hydrophobic Pro238 to hydrophilic Asp should cause large free energy loss for desolvation of Asp to maintain the same structure. To avoid this free energy loss, Asp238 showed a large shift out of its original position to achieve access to the solvent region. Additionally, the position of Pro238 in Fc(IgG1) was occupied by Leu235 instead in C_H2-A of Fc(P238D) complexed with FcγRIIb. As the result, the large conformational change of loop233–240 attached to the hinge region was observed. This change would affect the domain arrangement between the C_H2-A and B domains because both C_H2 domains connect by S–S bonds in the hinge region and cannot move independently. In fact, the relative arrangement of C_H2-A and B domains in the Fc(P238D)/FcγRIIb complex was different from that of Fc(IgG1)/FcγRIIa^{R131}, despite FcγRIIb having the highest homology to FcγRIIa^{R131}. As the result of these dynamic conformational changes, Fc(P238D) acquired two novel interactions with FcγRIIb. One is the hydrogen bond between the main chain of Gly237 in C_H2-A and the side chain of Tyr160 in FcγRIIb. Both FcγRIIa allotype cannot make this hydrogen bond because corresponding residue of this Tyr is Phe in FcγRIIa (Supplementary Fig. S1). So, this interaction would play a critical role for distinguishing FcγRIIb from FcγRIIa. The other one is the salt bridge between Asp270 in C_H2-A and Arg131 of FcγRIIb. This salt bridge would contribute to improve not only the binding affinity to FcγRIIb but also the selectivity over FcγRIIa^{H131} because this allotype has His as the corresponding residue of Arg131 in FcγRIIb. On the other hand, the S267E/L328F variant increased binding affinity to both FcγRIIb and FcγRIIa^{R131} to the same extent, while it did not increase binding affinity to FcγRIIa^{H131} or other FcγRs. From the reported complex structure of Fc(IgG1)/FcγRIIa^{R131}, we elucidated that Glu267 of the Fc with S267E/L328F substitution would form a salt bridge with Arg131 of the FcγRIIb and also of the FcγRIIa^{R131}. This might explain the reason for the lack of selectivity of the S267E/L328F variant to FcγRIIb over FcγRIIa^{R131}, both of which have Arg at position 131. Large conformational change induced by P238D would also explain the reason for lack of additive effect of combining P238D with L328E or S267E/L328F.

Then, in order to further increase the binding affinity to FcγRIIb, we conducted a second comprehensive mutagenesis using the P238D variant as a template rather than combining substitution(s) effective for wild-type IgG1 template, since the interface of Fc(P238D)/FcγRIIb was considered to be significantly changed from that of Fc(IgG1)/FcγRIIb. P238D-based comprehensive and combinatorial study identified V12 variant whose affinity for FcγRIIb was significantly increased from P238D variant. Especially, P271G markedly increased affinity for FcγRIIb. The substitution of fixed proline to flexible glycine would contribute to release conformational stress when a salt bridge between Asp270 in Fc (V12) and Arg131 in FcγRIIb is formed, which is considered to contribute to the affinity improvement for FcγRIIb.

Structural analysis of P238D suggests that P238D substitution seemed to destabilize the hydrophobic core of C_H2 domain, although this could be partially compensated by Leu235 as found in C_H2-A domain. The conformational changes seem to be the cause of decreased T_M for V12 variant. Although this reduced T_M raised concern regarding the storage stability of Fc(V12) for pharmaceutical application, its stability (aggregation tendency at 100 mg/ml) was comparable with that of wild-type IgG1.

It is known that, for IgG1 antibody to have a long half-life *in vivo*, binding to FcRn at acidic pH is important. The affinity of V12 variant for hFcRn was comparable with that of wild-type IgG1 and, consistently, the *in vivo* half-life of V12

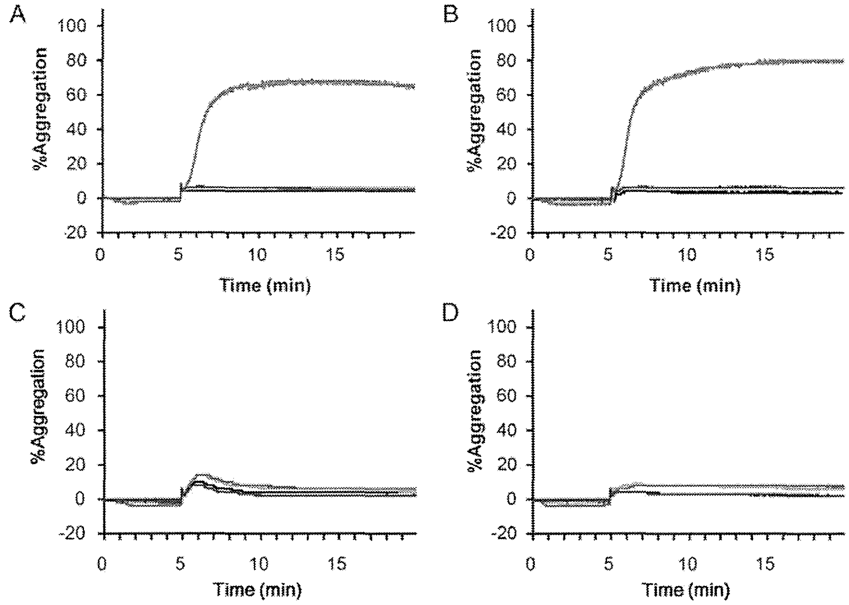

Fig. 6. Platelet aggregation studies incubated with ICs. Platelet aggregation was evaluated after platelets were incubated with ICs consisting of IgE with anti-IgE V12 variant (blue), that of anti-IgE S267E/L328F variant (red), IgE and anti-IgE IgG1 (green) or phosphate-buffered saline (black) for 5 min after being primed with ADP. Aggregation of the platelets from two donors with FcγRIIa R/R131 homozygous genotype are shown in panels **A** and **B**, respectively. Aggregation of the platelets from two donors with FcγRIIa H/H131 homozygous genotype are shown in panels **C** and **D**, respectively.

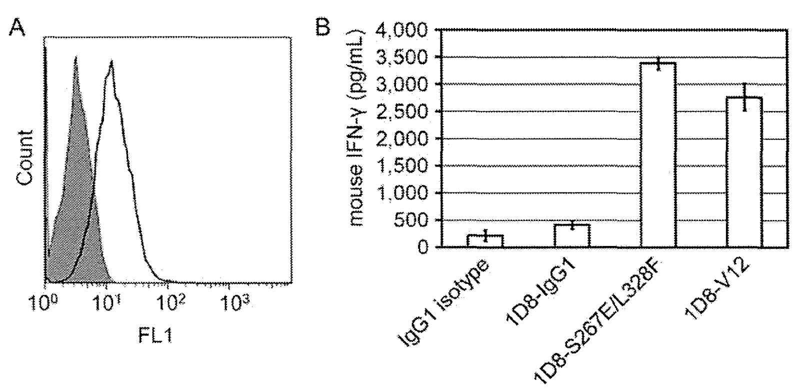

Fig. 7. V12 variant enhanced the T-cell activating agonistic activity of anti-CD137 antibody 1D8. (**A**) CD137 surface expression on CTLL-2 cells. Open histogram indicates 1D8-IgG1 and filled histogram indicates IgG1 isotype control. (**B**) T-cell activation induced by anti-CD137 antibody with different Fc (IgG1, V12 variant and S267E/L328F variant) was measured as mouse IFN-γ production of CTLL-2 co-cultured with Raji. Each bar shows mean ± SEM of three independent experiments.

variant was also comparable with that of wild-type IgG1. However, it should be noted that because the binding affinity of V12 variant to murine FcγRIIb (the mouse counterpart of human FcγRIIb) was not increased, its effect on the pharmacokinetics was not addressed in this study.

ICs induce platelet aggregation and activation when antibody binds to FcγRIIa expressed on the platelet surface (Boumpas *et al.*, 2003; Scappaticci *et al.*, 2007). The previous studies suggest that ICs consisting of IgG with enhanced binding to FcγRIIa have the potential to induce platelet aggregation and activation more intensively than IC consisting of wild-type IgG. However, the effect of engineered Fc with enhanced binding affinity to FcγRIIa on platelet activation and aggregation induced by IC has not so far been investigated. In this report, IC consisting of IgE and anti-IgE antibody with enhanced binding affinity to both FcγRIIb and $Fc\gamma RIIa^{R131}$ (S267E/L328F variant) induced the activation and aggregation of platelets obtained from FcγRIIa genotype of R/R131 homozygous donors, but not from FcγRIIa genotype of H/H131 homozygous donors. On the other hand, anti-IgE antibody with selectively enhanced binding affinity to FcγRIIb did not induce the activation or aggregation of platelets from donors with either genotype. Platelets whose FcγRIIa genotype is R/H131 are considered to express both FcγRIIa allotypes on their surface, while platelets whose FcγRIIa genotype is R/R131 express only $Fc\gamma RIIa^{R131}$. Therefore, a similar tendency will be observed in the platelets from heterozygous donors, although the induction of the aggregation and activation might be milder.

It is known that FcγRIIa internalizes ICs by endocytosis and transfers them to lysosomal degradation (Zhang and Booth, 2010), while FcγRIIb recycles the internalized ICs

(Bergtold *et al.*, 2005; Mousavi *et al.*, 2007). These reports suggest that an antibody with enhanced binding affinity to FcγRIIa would be more rapidly eliminated from plasma by FcγRIIa-mediated uptake and degradation than wild-type IgG1, while an antibody with enhanced binding only to FcγRIIb would have a longer half-life because the antibody would be recycled back to the cell surface. Indeed, an antibody with enhanced binding to both murine FcγRII and FcγRIII (counterpart of human FcγRIIa) exhibited more rapid clearance from plasma compared with an antibody with enhanced binding only to murine FcγRII (data not shown).

These facts indicate that therapeutic IgG with S267E/L328F substitution has the potential to induce platelet aggregation and activation and to be rapidly cleared from plasma in patients with FcγRIIa^{R131} genotype. One report described that the allelic frequency of R/R131, R/H131 and H/H131 is 31, 44 and 25%, respectively, among healthy Caucasians, and 26, 43 and 31%, respectively, among healthy African Americans (Lehrnbecher *et al.*, 1999). Another report showed that in Japanese, Chinese and Asian Indian populations the R/R131 genotype occurs in 6, 6 and 31%, respectively (Osborne *et al.*, 1994). Considering the proportion of populations with R/R and R/H genotypes, enhancing the binding affinity to FcγRIIa^{R131} would have a substantial impact.

Previous studies using S267E/L328F or S267E substitution(s) have demonstrated that enhancing affinity to FcγRIIb is a promising application for therapeutic antibodies against CD19, IgE, DR5 and CD40 (Li and Ravetch, 2011, 2012; Chu *et al.*, 2012; Hammer, 2012). Consistent with these reports, V12 variant, as well as S267E/L328F variant, enhanced agonistic activity of antibody against CD137, one of TNFR superfamily molecules, compared with intact human IgG1. Since agonistic antibodies against TNFR superfamily are currently being explored for cancer immunotherapy, enhancement of the agonistic activity of these antibodies by selectively improving the binding affinity for FcγRIIb could be a promising approach. In addition, in Ba/F3 cells expressing constitutively active mutants of the receptor tyrosine kinase, Kit, ICs that crosslinked FcγRIIb and Kit inhibited growth factor-independent proliferation (Malbec and Daëron, 2012). In another report, ICs suppressed the TLR4-mediated response of DCs in rheumatoid arthritis patients through FcγRIIb. Each of these effects of FcγRIIb could be enhanced by applying Fc with enhanced affinity for FcγRIIb. Moreover, ICs significantly suppressed expression of CD40, CD80 and CD86 on FcγRIIb-overexpressing DCs, suggesting that in DCs, using ICs consisting of an antibody variant with selectively enhanced FcγRIIb affinity relative to FcγRIIa might polarize IC-triggered activating signals to inhibitory signals (Zhang *et al.*, 2011).

Conclusion

In this study, we screened antibody Fc variant which selectively enhances the binding affinity to FcγRIIb over both FcγRIIa^{R131} and FcγRIIa^{H131} by comprehensive mutagenesis. We identified a distinct substitution, P238D, that could discriminate FcγRIIb from FcγRIIa^{R131} precisely, and crystal structural analysis revealed that this substitution substantially changed the recognition interface of Fc-FcγRIIb. We further designed an antibody variant with 200-fold higher affinity for FcγRIIb than IgG1 without increasing the affinity for other active FcγRs. The variant was comparable with IgG1 in terms of pharmacokinetics and storage stability. We also showed that an antibody with increased affinity for FcγRIIa has an increased possibility of inducing platelet activation and aggregation and of being rapidly cleared from plasma. Since previous studies and our study using agonist anti-CD137 antibody suggested that increasing the binding affinity to FcγRIIb has various therapeutic applications, our engineered Fc, which enhances binding selectivity to FcγRIIb, is expected to have a significant therapeutic potential.

Supplementary data

Supplementary data are available at *PEDS* online.

Acknowledgements

We thank our colleagues at Chugai Research Institute for Medical Science, Inc. and Chugai Pharmaceutical Co., Ltd: M.Fujii, Y.Nakata, A.Maeno and S.Masujima for antibody generation; W.Hatakeyama and M.Saito for carrying out SPR analysis; M.Irie for carrying out preparation of GST-EndoF1; R.Saito for carrying out platelet aggregation assay and A.Sakamoto, M.Okamoto and M.Endo for carrying out preparation of human FcγRs.

Funding

This work was fully supported by Chugai Pharmaceutical Co., Ltd. Funding to pay the Open Access publication charges for this article was provided by Chugai Pharmaceutical Co., Ltd.

References

Bergtold,A., Desai,D.D., Gavhane,A. and Clynes,R. (2005) *Immunity*, **23**, 503–514.
Boruchov,A.M., Heller,G., Veri,M.C., Bonvini,E., Ravetch,J.V. and Young,J.W. (2005) *J. Clin. Invest.*, **115**, 2914–2923.
Boumpas,D.T., Furie,R., Manzi,S., Illei,G.G., Wallace,D.J., Balow,J.E. and Vaishnaw,A.; BG9588 Lupus Nephritis Trial Group. (2003) *Arthritis Rheum.*, **48**, 719–727.
Brekke,O.H. and Sandlie,I. (2003) *Nat. Rev. Drug Discov.*, **2**, 52–62.
Cemerski,S., Chu,S.Y., Moore,G.L., Muchhal,U.S., Desjarlais,J.R. and Szymkowski,D.E. (2012) *Immunol. Lett.*, **143**, 34–43.
Chu,S.Y., Vostiar,I., Karki,S., Moore,G.L., Lazar,G.A., Pong,E., Joyce,P.F., Szymkowski,D.E. and Desjarlais,J.R. (2008) *Mol. Immunol.*, **45**, 3926–3933.
Chu,S.Y., Horton,H.M., Pong,E., *et al.* (2012) *J. Allergy Clin. Immunol.*, **129**, 1102–1115.
Crowley,J.E., Stadanlick,J.E., Cambier,J.C. and Cancro,M.P. (2009) *Blood*, **113**, 1464–1473.
Dall'Acqua,W.F., Cook,K.E., Damschroder,M.M., Woods,R.M. and Wu,H. (2006) *J. Immunol.*, **177**, 1129–1138.
DeLano,W.L. (2002) *The PyMOL Molecular Graphics System*. Palo Alto, CA, Schrödinger, LLC.
Desai,D.D., Harbers,S.O., Flores,M., Colonna,L., Downie,M.P., Bergtold,A., Jung,S. and Clynes,R. (2007) *J. Immunol.*, **178**, 6217–6226.
Emsley,P., Lohkamp,B., Scott,W.G. and Cowtan,K. (2010) *Acta Cryst.*, **D66**, 486–501.
Evans,P. (2006) *Acta Cryst.*, **D62**, 72–82.
Grueninger-Leitch,F., D'Arcy,A., D'Arcy,B. and Chène,C. (1996) *Protein Sci.*, **5**, 2617–2622.
Hammer,O. (2012) *mAbs*, **4**, 571–577.
He,F., Hogan,S., Latypov,R.F., Narhi,L.O. and Razinkov,V.I. (2010) *J. Pharm. Sci.*, **99**, 1707–1720.
Hernández,T., de Acosta,C.M., López-Requena,A., Moreno,E., Alonso,R., Fernández-Marrero,Y. and Pérez,R. (2010) *Mol. Immunol.*, **48**, 98–108.
Heyman,B. (2003) *Immunol. Lett.*, **88**, 157–161.
Horton,H.M., Chu,S.Y., Ortiz,E.C., *et al.* (2011) *J. Immunol.*, **186**, 4223–4233.
Igawa,T., Tsunoda,H., Tachibana,T., *et al.* (2010) *Protein Eng. Des. Sel.*, **23**, 385–392.
Kabsch,W. (2010) *Acta Cryst.*, **D66**, 125–132.

Lehrnbecher,T., Foster,C.B., Zhu,S., Leitman,S.F., Goldin,L.R., Huppi,K. and Chanock,S.J. (1999) *Blood*, **94**, 4220–4232.
Leibson,P.J. (2004) *Curr. Opin. Immunol.*, **16**, 328–336.
Li,F. and Ravetch,J.V. (2011) *Science*, **333**, 1030–1034.
Li,F. and Ravetch,J.V. (2012) *Proc. Natl Acad. Sci. USA*, **109**, 10966–10971.
Maggon,K. (2007) *Curr. Med. Chem.*, **14**, 1978–1987.
Malbec,O. and Daëron,M. (2012) *Immunol. Lett.*, **143**, 28–33.
McCoy,A.J., Grosse-Kunstleve,R.W., Adams,P.D., Winn,M.D., Storoni,L.C. and Read,R.J. (2007) *J. Appl. Crystallogr.*, **40**, 658–674.
Meyer,T., Robles-Carrillo,L., Robson,T., Langer,F., Desai,H., Davila,M., Amaya,M., Francis,J.L. and Amirkhosravi,A. (2009) *J. Thromb. Haemost.*, **7**, 171–181.
Mössner,E., Brünker,P., Moser,S., *et al.* (2010) *Blood*, **115**, 4393–4402.
Mousavi,S.A., Sporstøl,M., Fladeby,C., Kjeken,R., Barois,N. and Berg,T. (2007) *Hepatology*, **46**, 871–884.
Murshudov,G.N., Skubák,P., Lebedev,A.A., Pannu,N.S., Steiner,R.A., Nicholls,R.A., Winn,M.D., Long,F. and Vagin,A.A. (2011) *Acta Cryst.*, **D67**, 355–367.
Nimmerjahn,F. and Ravetch,J.V. (2005) *Science*, **310**, 1510–1512.
Nimmerjahn,F. and Ravetch,J.V. (2008) *Nat. Rev. Immunol.*, **8**, 34–47.
Nimmerjahn,F. and Ravetch,J.V. (2012) *Cancer Immun.*, **12**, 13.
Osborne,J.M., Chacko,G.W., Brandt,J.T. and Anderson,C.L. (1994) *J. Immunol. Methods*, **173**, 207–217.
Pollreisz,A., Assinger,A., Hacker,S., *et al.* (2008) *Br. J. Dermatol.*, **159**, 578–584.
Ramsland,P.A., Farrugia,W., Bradford,T.M., *et al.* (2011) *J. Immunol.*, **187**, 3208–3217.
Richards,J.O., Karki,S., Lazar,G.A., Chen,H., Dang,W. and Desjarlais,J.R. (2008) *Mol. Cancer Ther.*, **7**, 2517–2527.
Robles-Carrillo,L., Meyer,T., Hatfield,M., *et al.* (2010) *J. Immunol.*, **185**, 1577–1583.
Scappaticci,F.A., Skillings,J.R., Holden,S.N., *et al.* (2007) *J. Natl Cancer Inst.*, **99**, 1232–1239.
Shuford,W.W., Klussman,K., Tritchler,D.D., *et al.* (1997) *J. Exp. Med.*, **186**, 47–55.
Smith,P., DiLillo,D.J., Bournazos,S., Li,F. and Ravetch,J.V. (2012) *Proc. Natl Acad. Sci. USA*, **109**, 6181–6186.
Stavenhagen,J.B., Gorlatov,S., Tuaillon,N., *et al.* (2007) *Cancer Res.*, **67**, 8882–8890.
White,A.L., Chan,H.T., Roghanian,A., *et al.* (2011) *J. Immunol.*, **187**, 1754–1763.
White,A.L., Chan,H.T., French,R.R., Beers,S.A., Cragg,M.S., Johnson,P.W. and Glennie,M.J. (2013) *Cancer Immunol Immunother.*, **62**, 941–948.
Wilson,N.S., Yang,B., Yang,A., *et al.* (2011) *Cancer Cell*, **19**, 101–113.
Winter,G. (2010) *J. Appl. Cryst.*, **43**, 186–190.
Zalevsky,J., Leung,I.W., Karki,S., Chu,S.Y., Zhukovsky,E.A., Desjarlais,J.R., Carmichael,D.F. and Lawrence,C.E. (2009) *Blood*, **113**, 3735–3743.
Zhang,C.Y. and Booth,J.W. (2010) *J. Biol. Chem.*, **285**, 34250–34258.
Zhang,Y., Liu,S., Yu,Y., Zhang,T., Liu,J., Shen,Q. and Cao,X. (2011) *Eur. J. Immunol.*, **41**, 1154–1164.

Engineered Monoclonal Antibody with Novel Antigen-Sweeping Activity *In Vivo*

Tomoyuki Igawa*, Atsuhiko Maeda, Kenta Haraya, Tatsuhiko Tachibana, Yuki Iwayanagi, Futa Mimoto, Yoshinobu Higuchi, Shinya Ishii, Shigero Tamba, Naoka Hironiwa, Kozue Nagano, Tetsuya Wakabayashi, Hiroyuki Tsunoda, Kunihiro Hattori

Research Division, Chugai Pharmaceutical Co., Ltd., Gotemba, Shizuoka, Japan

Abstract

Monoclonal antibodies are widely used to target disease-related antigens. However, because conventional antibody binds to the antigen but cannot eliminate the antigen from plasma, and rather increases the plasma antigen concentration by reducing the clearance of the antigen, some clinically important antigens are still difficult to target with monoclonal antibodies because of the huge dosages required. While conventional antibody can only bind to the antigen, some natural endocytic receptors not only bind to the ligands but also continuously eliminate them from plasma by pH-dependent dissociation of the ligands within the acidic endosome and subsequent receptor recycling to the cell surface. Here, we demonstrate that an engineered antibody, named sweeping antibody, having both pH-dependent antigen binding (to mimic the receptor-ligand interaction) and increased binding to cell surface neonatal Fc receptor (FcRn) at neutral pH (to mimic the cell-bound form of the receptor), selectively eliminated the antigen from plasma. With this novel antigen-sweeping activity, antibody without *in vitro* neutralizing activity exerted *in vivo* efficacy by directly eliminating the antigen from plasma. Moreover, conversion of conventional antibody with *in vitro* neutralizing activity into sweeping antibody further potentiated the *in vivo* efficacy. Depending on the binding affinity to FcRn at neutral pH, sweeping antibody reduced antigen concentration 50- to 1000-fold compared to conventional antibody. Thereby, sweeping antibody antagonized excess amounts of antigen in plasma against which conventional antibody was completely ineffective, and could afford marked reduction of dosage to a level that conventional antibody can never achieve. Thus, the novel mode of action of sweeping antibody provides potential advantages over conventional antibody and may allow access to the target antigens which were previously undruggable by conventional antibody.

Citation: Igawa T, Maeda A, Haraya K, Tachibana T, Iwayanagi Y, et al. (2013) Engineered Monoclonal Antibody with Novel Antigen-Sweeping Activity *In Vivo*. PLoS ONE 8(5): e63236. doi:10.1371/journal.pone.0063236

Editor: Maria Gasset, Consejo Superior de Investigaciones Cientificas, Spain

Received October 31, 2012; **Accepted** April 1, 2013; **Published** May 7, 2013

Funding: The authors have no support or funding to report.

Competing Interests: All authors are employees of Chugai Pharmaceutical Co., Ltd. T.I. and A.M. are inventors of the patents which claim pH-dependent binding antibody and sweeping antibody. This does not alter the authors' adherence to all the PLOS ONE policies on sharing data and materials.

* E-mail: igawatmy@chugai-pharm.co.jp

Introduction

Therapeutic monoclonal antibodies are now becoming an important option for treating various diseases [1,2]. Although high affinity antibodies with neutralizing activity against various antigens have been generated and shown to be therapeutically effective *in vivo*, some clinically important antigens have proved difficult to target by conventional antibody because of the huge antibody dosage required.

It has been reported that administering conventional antibodies to target soluble antigens, such as amyloid beta [3], MCP1 [4], hepcidin [5], IL6 [6], CD23 [7] and VEGF [8], results in more than 1000-fold increased antigen concentration over the baseline due to the accumulation of antibody-antigen complex in plasma. Since the half-life of the IgG antibody is very much longer than that of the antigen, the binding of antigen to antibody results in an increase in the plasma antigen concentration by reducing the clearance of the antigen [9]. The extent of increase in antigen concentration is determined by the difference in clearance between antigen and antibody-antigen complex [10]. As a striking example, administration of high affinity antibody against hepcidin, which has very rapid clearance, resulted in approximately 5,000-fold increase in plasma hepcidin concentration, requiring a huge antibody dosage of 300 mg/kg weekly to neutralize the hepcidin, which is an unrealistic dosage for therapeutic development [5]. In other cases, the baseline plasma concentration of the antigen may itself be extremely high, as in that of complement factor C5, the target antigen of eculizumab, which is in the range of μg/mL, in contrast to most therapeutic antibodies in the pg/mL or ng/mL range. Because of such high C5 concentration, eculizumab requires huge antibody dosage for efficient C5 neutralization [11], which makes eculizumab one of the highest annual dosages of the approved therapeutic antibodies. In theory, even an antibody with infinite affinity would need to be at a concentration higher than that of the total antigen to neutralize that antigen *in vivo* [12]. Therefore, when targeting soluble antigens with rapid clearance or high baseline plasma concentration, even conventional antibody with infinite affinity requires huge antibody dosage to achieve therapeutic efficacy. This impedes not only the development of subcutaneous formulations, which are important for chronic disease, but also the commercial development itself, because of increased manufacturing cost.

Since these issues stem from the fact that conventional antibody can only bind to the antigen and accumulates the antigen in plasma, engineered antibody that enables active and selective elimination of the antigen from plasma could overcome these issues. In the natural system, several cell surface endocytic receptors, such as asialoglycoprotein receptor [13], low-density lipoprotein receptor [14] and epidermal growth factor receptor [15], deliver ligands to the lysosome to eliminate the ligands from plasma. These receptors bind to the ligands at the cell surface and internalize the ligands into the cell. Since these receptors bind to the ligands pH dependently, they release the ligands in the acidic endosome, and while the released ligands are transferred to lysosome and degraded, the free receptors rapidly recycle back to the cell surface for another round of ligand elimination from plasma. Such properties make these receptors ideal for "sweeping" the ligands from the plasma. In this study, we engineered monoclonal antibody to mimic the endocytic receptor-like property so that it can exert antigen-sweeping activity and eliminate the antigen from the plasma.

We have investigated engineered monoclonal antibody to exert novel antigen-sweeping activity by simultaneously engineering both pH-dependent antigen binding, to mimic the pH-dependent receptor-ligand binding of such endocytic receptors, and increased FcRn binding affinity at neutral pH, to mimic the cell-bound form of the receptors. We demonstrate that the conversion of conventional antibody into sweeping antibody, which directly eliminates the antigen from plasma, could afford huge reduction of the antibody dosage to a level that conventional antibody even with infinite affinity cannot achieve and may allow access to target antigens which have previously been undruggable by conventional antibody.

Materials and Methods

Ethics Statement

Animal studies were performed in accordance with the Guidelines for the Care and Use of Laboratory Animals at Chugai Pharmaceutical Co., Ltd. under the approval of the company's Institutional Animal Care and Use Committee. The company is fully accredited by the Association for Assessment and Accreditation of Laboratory Animal Care International (http://www.aaalac.org).

Generation of Anti-IL-6R Antibodies with Increased Binding Affinity to FcRn at Neutral pH

pH-dependent binding antibody against human soluble IL-6 receptor (hsIL-6R) with neutralizing activity (PH-IgG1) were generated from non-pH-dependent binding antibody (NPH-IgG1) as previously described [16]. pH-dependent binding antibodies against hsIL-6R without neutralizing activity (PHX-IgG1) in BaF/gp130 assay [17] were also generated. To increase the binding affinity to either mouse FcRn (mFcRn) or human FcRn (hFcRn) at neutral pH, various Fc-engineered variants were generated by site-directed mutagenesis of human IgG1. Amino acid substitutions were introduced at the positions 251–258, 286, 288, 307–316, 428 and 433–436 in the EU numbering system which were reported to affect FcRn binding [18–26]. Mutation was comprehensively introduced at each position, and effective mutations identified were combined to generate Fc variants with increased binding affinity to FcRn at neutral pH. More than 1,000 variants were generated and assessed for their binding affinity (K_D) to recombinant mFcRn or hFcRn [18] at pH 7.0 using Biacore T200 (GE Healthcare). Each variant was captured onto a Protein L (ACTIgen) immobilized CM4 sensor chip, then FcRn was injected over the flow cell. K_D was determined using Biacore T200 Evaluation Software (GE Healthcare). Fc variants with the desired affinity to FcRn were identified. NPH-IgG1 (conventional antibody with neutralizing activity but without pH-dependent binding), PH-IgG1, PHX-IgG1 and their Fc variants were expressed transiently and purified. NPH-IgG1, PH-IgG1 and PHX-IgG1 were assessed for their K_D to recombinant hsIL-6R at pH 7.4 and pH 6.0 as previously described [16].

In vivo Study of Antibodies in Normal Mice and hFcRn Transgenic Mice Co-injection Model

All animal experiments in this study were performed in accordance with the Guidelines for the Care and Use of Laboratory Animals at Chugai Pharmaceutical Co., Ltd. In co-injection model, C57BL/6J normal mice (Charles River) or hFcRn transgenic mice (hFcRn-Tgm, B6.mFcRn−/−.hFcRn Tg line 276+/+ mouse, Jackson Laboratories) [27] were administered by single i.v. injection with hsIL-6R alone or with hsIL-6R pre-mixed with antibody. The first group received 50 μg/kg hsIL-6R but the other groups additionally received 1 mg/kg of anti-IL-6R antibodies. Total hsIL-6R plasma concentration was determined as previously described [16].

In vivo Study of Antibodies in a Normal Mice hsIL-6R Trans-signaling Model

To evaluate the effect of antibodies on hsIL-6R trans-signaling inhibition *in vivo*, C57BL/6J normal mice were initially i.v. injected with hsIL-6R [16] (250 μg/kg). Then antibodies with designated doses and MR16-1 [28] (15 mg/kg, rat anti-mouse IL-6R antibody) were administered at 2 h after the initial injection. 8 μg/kg of human IL-6 (Toray) was injected at 24 h. Blood samples were collected at 30 h after the initial injection and total hsIL-6R and serum amyloid A (SAA) plasma concentrations were determined as previously described [16].

In vivo Study of Single Doses of Antibodies in Normal Mice and hFcRn Transgenic Mice Steady-state Model

An infusion pump (alzet) filled with 92.8 μg/mL hsIL-6R was implanted under the skin on the back of C57BL/6J normal mice or hFcRn-Tgm (B6.mFcRn−/−.hFcRn Tg line 32+/+ mouse, Jackson Laboratories) [27] to prepare model mice with constant plasma concentration of hsIL-6R. Monoclonal anti-mouse CD4 antibody GK1.5 [29] was administered by i.v. injection to inhibit the production of mouse antibody against hsIL-6R by depleting CD4+ T-cells. Antibodies against hsIL-6R were administered at 1 mg/kg to normal mice or hFcRn-Tgm with or without a single i.v. injection of 1 g/kg of hIgG (Intravenous immunoglobulin, CSL Behring) to mimic endogenous human IgG.

Plasma anti-hsIL-6R antibody concentration in the presence of human IgG was determined using anti-idiotype antibody coated on ELISA 96-well plates, and detected by hsIL-6R, biotinylated anti-hIL-6R antibody (R&D Systems) and Streptavidin-PolyHRP80 (Stereospecific Detection Technologies) using peroxidase substrate. Plasma total hsIL-6R, antibody concentration in the absence of hIgG and pharmacokinetic parameters were determined as previously described [16]. The theoretical free hsIL-6R concentration was calculated from antibody concentration, total hsIL-6R concentration and the K_D of the antibody by equilibrium reaction formula.

In vivo Study of Multiple Doses of Antibodies in hFcRn Transgenic Mice Steady-state Model with High hsIL-6R Concentration

Study was performed as described in the single dose study but with 320 μg/mL hsIL-6R in the pump, and doses were administered to hFcRn-Tgm (B6.mFcRn−/−.hFcRn Tg line 32+/+ mouse, Jackson Laboratories) [27] every other day (except the first dose which was injected together with a single i.v. injection of 1 g/kg of human IgG). Total hsIL-6R plasma concentrations were determined as described above. To determine free hsIL-6R plasma concentration, samples were treated by rProtein A (GE healthcare) to remove antibody and antibody-antigen complex. Because rProtein A treatment requires 10 μL of plasma, samples of $n = 3–5$ were equally pooled before the treatment. Subsequently, the free hsIL-6R plasma concentrations were determined by the same method as for total hsIL-6R, and hsIL-6R neutralization percentages were obtained by calculating the percentage reduction of free hsIL-6R plasma concentration over control group.

Pharmacokinetic Analysis and Simulation using Antibody-antigen Dynamic Model

The plasma concentration–time profiles of antibodies and total hsIL-6R obtained in the study of hFcRn-Tgm steady-state model were fitted to an antibody-antigen dynamic model [30] and parameters were optimized for conventional, pH-dependent binding, and v4-type sweeping antibodies. The k_a and k_d values were from surface plasmon resonance (SPR) data. Simulation study was carried out using the obtained pharmacokinetic parameters, and antibody dosages required to neutralize 95% of the antigen (baseline 250 ng/mL (6.6 nM)) at trough by dosing once a month were obtained for each type of antibody with antigen binding affinity (K_D) of 0.001, 0.01, 0.1, 1 and 10 nM.

Results

Antigen Sweeping by pH-dependent Binding Antibody with Increased FcRn Binding at Neutral pH

In order to evaluate the effect of pH-dependent antigen binding and increased FcRn binding affinity at neutral pH on antigen pharmacokinetics, we used a non-pH-dependent binding antibody against hsIL-6R with hIgG1 constant region (NPH-IgG1) and a pH-dependency-engineered variant (PH-IgG1) (Table S1). hIgG1 has almost no detectable binding to FcRn at pH 7.4, and very weak binding at pH 7.0. In order to increase the binding affinity of PH-IgG1 to either mouse FcRn (mFcRn) or human FcRn (hFcRn) at neutral pH, various hIgG1 Fc variants with mutation(s) in the FcRn binding region (positions 251–258, 286, 288, 307–316, 428 and 433–436 in the EU numbering system) were generated by site-directed mutagenesis. More than 1000 variants were screened by binding to either mFcRn or hFcRn at pH 7.0, and hIgG1 Fc variants for *in vivo* studies were selected (Table 1). The v1 variant was used to evaluate the *in vivo* effect of pH-dependent antigen binding antibody with increased binding affinity to mFcRn at pH 7.0 by administering hsIL-6R to normal mice either on its own or in complex with NPH-IgG1, PH-IgG1 or PH-v1 (Fig. 1A). In this co-injection model, NPH-IgG1 significantly reduced the clearance of hsIL-6R because antigen-antibody complex has lower clearance than the antigen [9,10]; PH-IgG1 increased the clearance of hsIL-6R to some extent, but was still slower than hsIL-6R alone; while PH-v1 accelerated the clearance of hsIL-6R faster than hsIL-6R alone.

Since this co-injection model may not have reflected the actual therapeutic situation where antibody is exposed to plasma in which steady-state baseline concentration of soluble antigen is present, we evaluated antigen sweeping in a mouse model which maintains steady-state plasma antigen concentration. We administered NPH-IgG1, PH-IgG1 and PH-v1 into normal mice steady-state model (Fig. 1B). Consistent with the co-injection model, NPH-IgG1 significantly increased hsIL-6R plasma concentration; PH-IgG1 reduced that increase but an increase over the baseline was still observed; and PH-v1 actively eliminated hsIL-6R from the plasma and reduced the plasma hsIL-6R concentration approximately 150-fold below the baseline, demonstrating that engineered antibody with pH-dependent binding antibody and increased binding affinity to FcRn at neutral pH can eliminate the antigen form plasma *in vivo*.

Effect of Antigen Sweeping by Sweeping Antibody on Antigen Antagonism *in vivo*

To evaluate the effect of antigen sweeping by sweeping antibody on antigen antagonism *in vivo*, *in vivo* efficacy of the anti-hsIL-6R sweeping antibodies was tested in a normal mouse hsIL-6R trans-signaling model [31], which exhibits an increase in SAA dependent on hIL-6/hsIL-6R-mediated trans-signaling. We generated PHX-IgG1, a pH-dependent binding antibody against hsIL-6R without hsIL-6R neutralizing activity *in vitro* (Table S1), and its Fc variant PHX-v1 with increased binding affinity to mFcRn at neutral pH. In the first study, PHX-IgG1 and PHX-v1 were administered at antibody dosage of 30 mg/kg, and plasma concentration of hsIL-6R and SAA, as a pharmacodynamic marker of hsIL-6R antagonism, are shown (Fig. 2A,B). While PHX-IgG1 could not inhibit SAA production at all, PHX-v1 significantly inhibited SAA production *in vivo* by directly sweeping hsIL-6R from the plasma, despite having no neutralizing activity *in vitro*. In the next study, antibodies with hsIL-6R neutralizing activity, NPH-IgG1, PH-IgG1 and PH-v1, were administered at antibody dosage of 0.03 mg/kg. While NPH-IgG1 and PH-IgG1 with hsIL-6R neutralizing activity *in vitro* could not completely inhibit SAA production at this dosage, PH-v1, with both neutralizing and sweeping activity, completely inhibited SAA production (Fig. 2C,D).

Antigen Sweeping Requires Both pH-Dependent Antigen Binding and Increased FcRn Binding Affinity at Neutral pH

For clinical application of sweeping antibody, further studies of antigen sweeping were conducted using an hFcRn system. The v2 variant with increased binding affinity to hFcRn at neutral pH was generated (Table 1). As a control for v2 variant, a YTE variant previously reported as improving the half-life [19] with increased binding affinity to hFcRn at acidic pH but not significantly at neutral pH, was used. In a co-injection model, hsIL-6R was administered to hFcRn-Tgm either on its own or in complex with NPH-IgG1, PH-IgG1, PH-YTE and PH-v2 (Fig. 3A). Consistent with the study using normal mice, PH-v2 markedly accelerated the clearance of hsIL-6R faster than hsIL-6R alone in hFcRn-Tgm. On the other hand, PH-YTE exerted slightly slower clearance of hsIL-6R than PH-IgG1.

To further clarify the molecular requirement to achieve antigen sweeping, we administered NPH-IgG1, PH-IgG1, NPH-v2, PH-v2 and PH-v0 to hFcRn-Tgm steady-state model (Fig. 3B). NPH-v2, a non-pH-dependent binding antibody with increased binding affinity to hFcRn at neutral pH, increased hsIL-6R plasma concentration above the baseline to a similar level to NPH-IgG1;

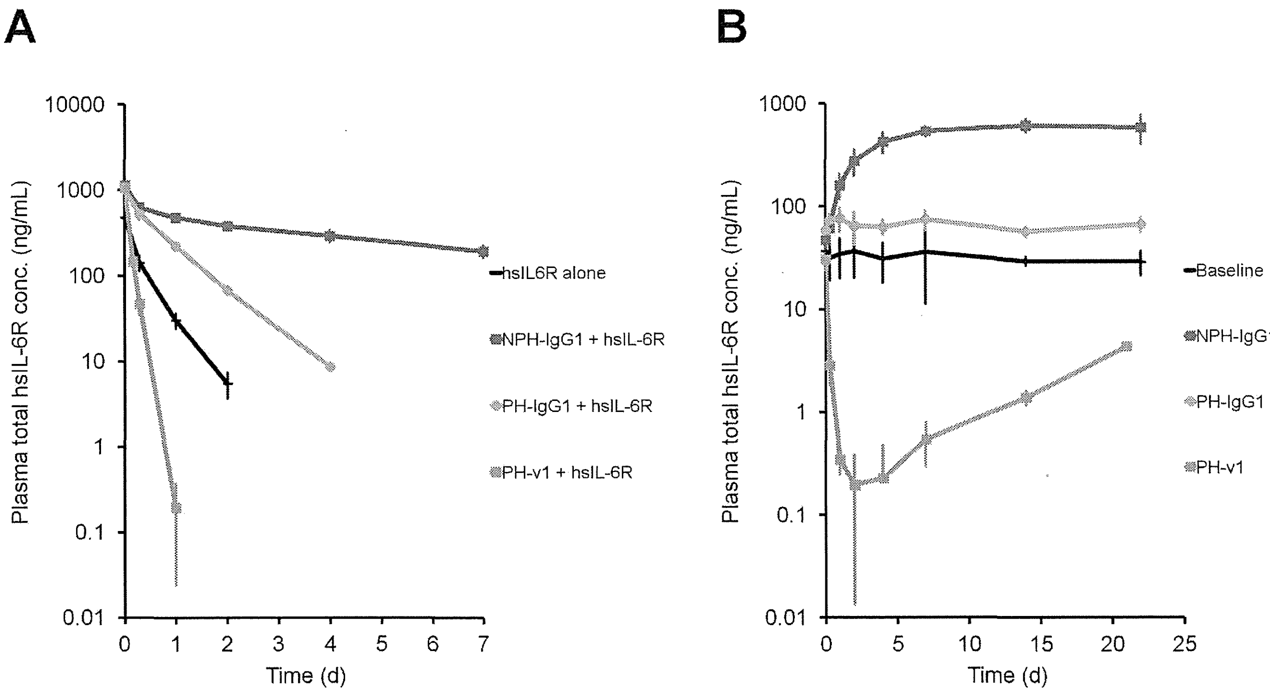

Figure 1. Antigen sweeping by pH-dependent antigen binding antibody with increased FcRn binding at neutral pH. *In vivo* study of NPH-IgG1, PH-IgG1 and PH-v1 in normal mice. Effect of antibodies on the total hsIL-6R plasma concentration was evaluated in a co-injection model and a steady-state model. In the co-injection model, hsIL-6R, hsIL-6R+NPH-IgG1, hsIL-6R+PH-IgG1 and hsIL-6R+PH-v1 were intravenously administered as single doses of 50 µg/kg for hsIL-6R and 1 mg/kg for antibody and a time profile of total hsIL-6R plasma concentration (A) is shown. Each data point represents the mean ± s.d. (n = 3 each). In the steady-state model, steady-state plasma concentration of approximately 20 ng/mL hsIL-6R was maintained using an infusion pump filled with hsIL-6R solution, and NPH-IgG1, PH-IgG1 and PH-v1 were intravenously administered as single doses of 1 mg/kg and a time profile of total hsIL-6R plasma concentration (B) is shown. Each data point represents the mean ± s.d. (n = 3 each).
doi:10.1371/journal.pone.0063236.g001

PH-v0, a pH-dependent binding antibody with no hFcRn binding [32], also increased hsIL-6R plasma concentration to a similar level to PH-IgG1, but only transiently; and only PH-v2, a pH-dependent binding antibody with increased binding affinity to hFcRn at neutral pH, actively eliminated hsIL-6R from the plasma. This clearly demonstrates that both pH-dependent antigen binding and increased binding affinity to FcRn at neutral pH are required for antigen sweeping.

Effect of Endogenous IgG Competition on Antigen Sweeping

Because mouse IgG does not bind to hFcRn [33], hFcRn-Tgm has substantially no endogenous IgG competing with sweeping antibody for hFcRn, which might not reflect the clinical situation in which there is high endogenous human IgG (hIgG) concentration [20]. To evaluate the effect of endogenous IgG on antigen sweeping, NPH-IgG1, PH-IgG1 and PH-v2 alone or together with

Table 1. Mutations and FcRn binding affinity of hIgG1 Fc variants.

Fc variant	K_D (nM) at pH7.0		K_D (nM) at pH6.0		Mutations
	mouse FcRn	human FcRn	mouse FcRn	human FcRn	
IgG1	3918	88000	237	1377	-
v1	52	NT	3	NT	I332V/N434Y
v2	NT	155	NT	6	M252W/N434W
v3	NT	288	NT	15	M252Y/N434Y
v4	NT	120	NT	8	M252Y/N286E/N434Y
v5	NT	77	NT	5	M252Y/T307Q/Q311A/N434Y
v6	NT	35	NT	3	M252Y/V308P/N434Y
v0	no binding	no binding	no binding	no binding	I253A

Binding affinity (K_D) of IgG1 and v1 to mFcRn at pH 7.0 and pH 6.0, binding affinity (K_D) of IgG1, v2-v6 and v0 to hFcRn at pH 7.0 and pH 6.0, and mutations introduced in the Fc region are shown. Mutation sites in the Fc region are described in EU numbering. NT, not tested.
doi:10.1371/journal.pone.0063236.t001

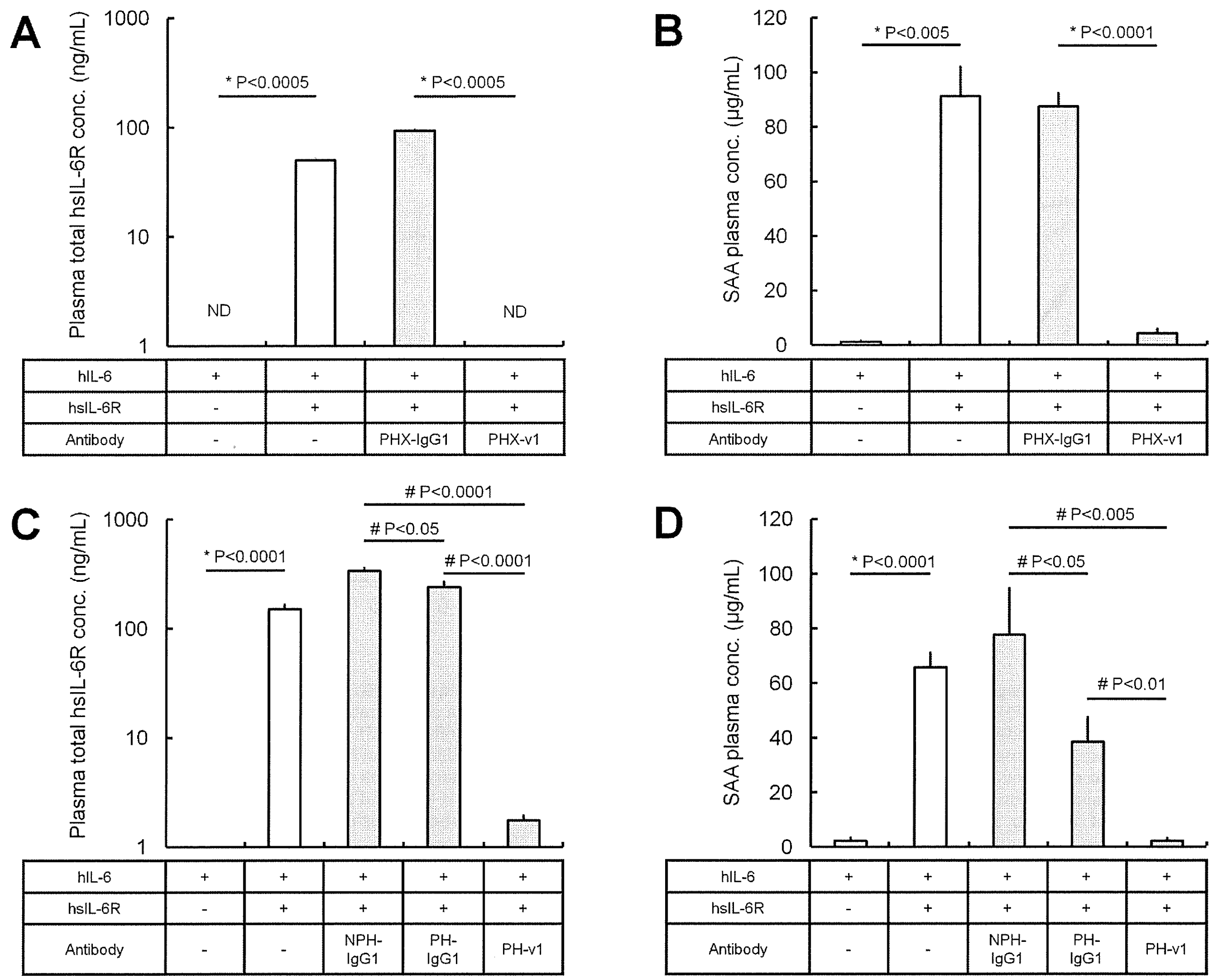

Figure 2. *In vivo* study of sweeping antibodies in a normal mice hsIL-6R trans-signaling model. Effect of antibodies on the total hsIL-6R plasma concentration and SAA plasma concentration (as a marker for hsIL-6R antagonism) were evaluated. hsIL-6R was intravenously administered as a single dose of 250 μg/kg. At 2 h, non-neutralizing antibodies PHX-IgG1 and PHX-v1 were intravenously administered as single doses of 30 mg/kg (A, B), and neutralizing antibodies NPH-IgG1, PH-IgG1 and PH-v1 were intravenously administered as single doses of 0.03 mg/kg (C, D). At 24 h, hIL-6 was intravenously administered as a single dose of 8 μg/kg. Total hsIL-6R plasma concentration (A, C) and SAA plasma concentration (B, D) at 30 h is shown. Each data represents the mean ± s.d. for total hsIL-6R plasma concentration and the mean ± s.e. for SAA plasma concentration (n = 3–7 each). ND, not detected (below 0.195 ng/mL). Statistical significance was determined by t-test (*) or Tukey's multiple comparison test (#) for total hsIL-6R and SAA plasma concentration.
doi:10.1371/journal.pone.0063236.g002

1 g/kg of hIgG, which mimics endogenous IgG, were administered to hFcRn-Tgm steady-state model. hsIL-6R sweeping by PH-v2 was attenuated when hIgG as endogenous IgG was present (Fig. S1).

Effect of hFcRn Binding Affinity at Neutral pH on Antigen Sweeping in Human FcRn Transgenic Mice

Since FcRn binding at neutral pH is required for antigen sweeping, it is assumed that binding affinity (K_D) to FcRn at neutral pH would affect the antigen sweeping profile. In addition, previous studies have shown that increasing FcRn binding affinity at neutral pH either increased or did not affect the antibody clearance [21–24]. In order to assess the effect of FcRn binding affinity at neutral pH on antigen sweeping and antibody pharmacokinetics, Fc variants (v3-v6) with various binding affinity to hFcRn at pH 7.0 were generated (Table 1).

Antigen sweeping and antibody pharmacokinetics of NPH-IgG1, PH-IgG1 and its Fc variants were evaluated in hFcRn-Tgm steady-state model in the presence of hIgG (Fig. 4A,B, Table S2). Compared to IgG1, the v3 variant, with K_D 288 nM at pH 7.0, slightly prolonged the antibody pharmacokinetics; moreover, PH-v3 reduced total hsIL-6R plasma concentration to a similar level as baseline concentration. Notably, the v4 variant, with K_D 120 nM at pH 7.0, reduced total hsIL-6R plasma concentration below the baseline level while the antibody pharmacokinetics was maintained. Total hsIL-6R plasma concentration of PH-v4 was 50-fold lower than NPH-IgG1 while the antibody plasma concentration was comparable. The study using the v5 and v6 variants with, respectively, K_D 77 and 35 nM at pH 7.0 has demonstrated that variants with stronger hFcRn binding affinity exhibited more

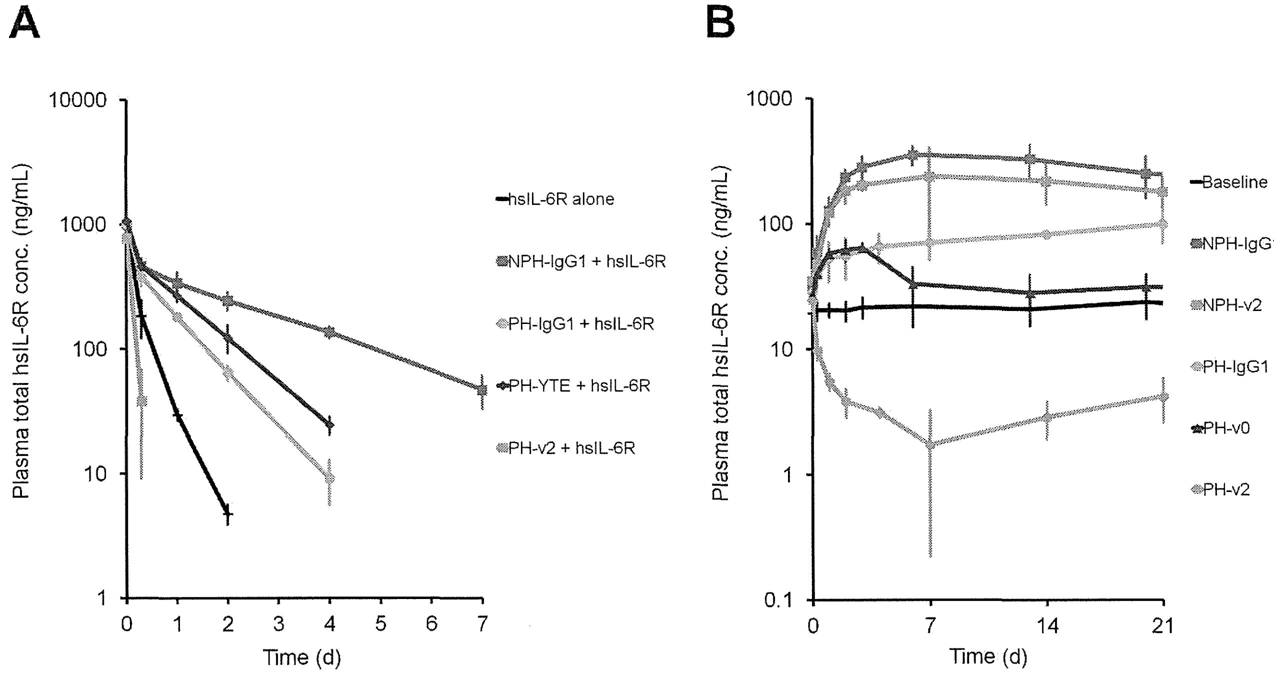

Figure 3. Characterization of sweeping antibody in hFcRn-Tgm. (A) *In vivo* study of NPH-IgG1, PH-IgG1, PH-YTE and PH-v2 in hFcRn-Tgm. Effect of antibodies on the total hsIL-6R plasma concentration was evaluated in a co-injection model. hsIL-6R, hsIL-6R+NPH-IgG1, hsIL-6R+PH-IgG1, hsIL-6R+PH-YTE and hsIL-6R+PH-v2 were intravenously administered as single doses of 50 µg/kg for hsIL-6R and 1 mg/kg for antibody and a time profile of total hsIL-6R plasma concentration is shown. Each data point represents the mean ± s.d. (n = 3 each). (B) Effect of pH-dependent antigen binding and increased binding affinity to FcRn at neutral pH on antigen sweeping in hFcRn-Tgm steady-state model with hsIL-6R plasma concentration of approximately 20 ng/mL. NPH-IgG1, NPH-v2, PH-IgG1, PH-v2 and PH-v0 were intravenously administered as single doses of 1 mg/kg. Time profile of total hsIL-6R plasma concentration is shown. Each data point represents the mean ± s.d. (n = 3 each).
doi:10.1371/journal.pone.0063236.g003

extensive antigen sweeping and lower minimum total hsIL-6R plasma concentration, but had increased antibody clearance and a shorter duration of antigen sweeping (faster recovery to baseline). Specifically, the v6 variant reduced total hsIL-6R plasma concentration approximately 1000-fold compared to NPH-IgG1, while the antibody clearance was increased only by 4-fold.

Sweeping Antibody Antagonizes High Concentration Antigen where Conventional Antibody is Ineffective

The v6-type sweeping antibody with hFcRn binding affinity of 35 nM provided short-lasting but extensive 1000-fold reduction of antigen plasma concentration compared to conventional antibody. To understand its therapeutic advantage, NPH-IgG1, PH-IgG1 and PH-v6 at doses of 0.01 mg/kg were administered to hFcRn-Tgm steady-state model with high plasma hsIL-6R concentration (250 ng/mL) every other day in the presence of hIgG (Fig. 5 A, B). Multiple dosing of NPH-IgG1 and PH-IgG1 achieved no hsIL-6R neutralization throughout the study because molar hsIL-6R concentration was higher than that of antibody (molar antibody concentration was approximately 5-fold lower than the total antigen concentration immediately after the first administration); however, PH-v6 gradually reduced the total hsIL-6R plasma concentration, enabling a neutralization of hsIL-6R at Day 8.

Discussion

In this study, we have demonstrated that simultaneous engineering of pH-dependent antigen binding and increased FcRn binding affinity at neutral pH actively eliminated the antigen from the plasma, creating "sweeping antibody". Importantly, both pH-dependent antigen binding and increased FcRn binding affinity at neutral pH was required for antigen sweeping, mimicking the function of the ligand-sweeping endocytic receptors that we previously mentioned.

When targeting soluble antigen with monoclonal antibody, conventional antibody (NPH-IgG1) remains bound to the soluble antigen within the acidic endosome (Fig. S2A) and thereby inhibits the antigen degradation by lysosome, resulting in accumulation of the antigen in the plasma. We have recently reported that engineered antibody with pH-dependent antigen binding (PH-IgG1), named recycling antibody, dissociates the soluble antigen in the acidic endosome and the dissociated antigen is then transferred to lysosome and degraded (Fig. S2B) [16]. However, our current study demonstrates that pH-dependent antigen binding alone could not actively eliminate the antigen from plasma. This is because intact IgG1 does not bind to FcRn on the cell surface at neutral pH [25], and the antibody-antigen complex is only marginally taken up into the cell by pinocytosis, which limits the rate of antigen degradation.

Previous studies have demonstrated that Fc-engineering to increase the binding affinity to FcRn at acidic pH improved the endosomal recycling efficiency and prolonged the pharmacokinetics of the antibody [20,25,26]. However, a simultaneous increase of binding affinity at neutral pH did not prolong [21,22], or even shortened [23,24], the pharmacokinetics because of inefficient antibody release from FcRn back to plasma after transporting it back to the cell surface, providing no therapeutic merit. Increasing FcRn binding affinity at neutral pH would anchor the antibody to the cell surface, similarly to an endocytic receptor, and enhance cellular uptake of antibody-antigen complex by FcRn-mediated

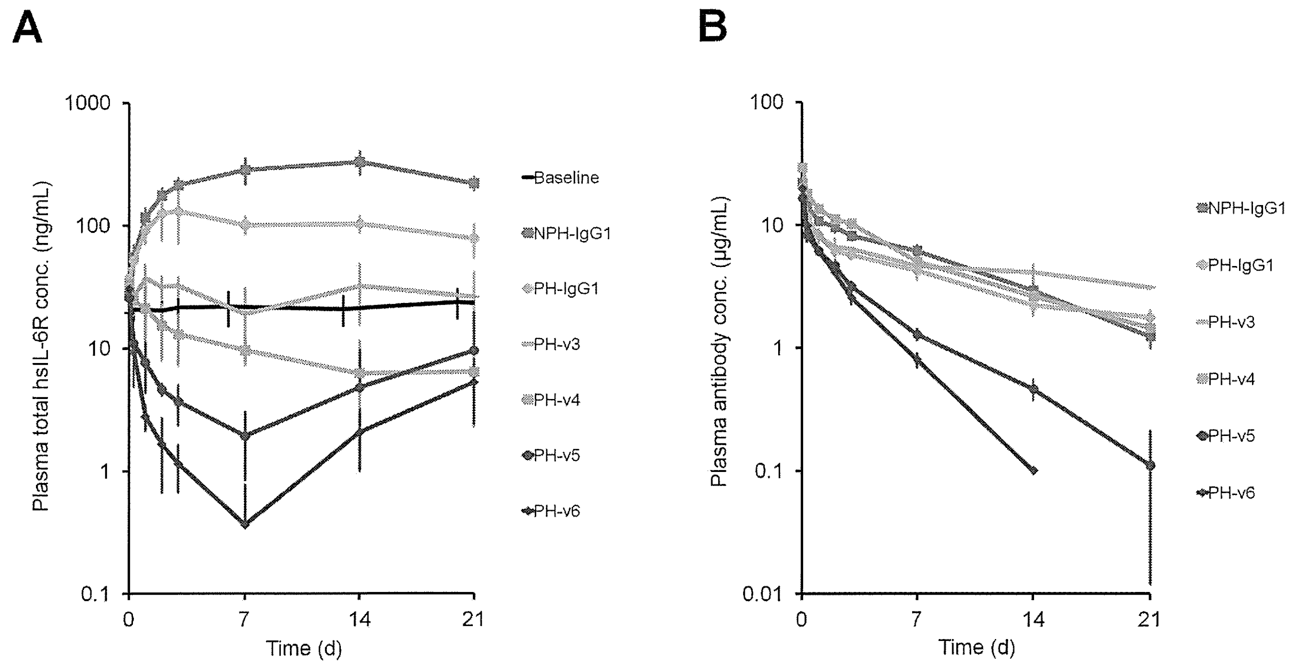

Figure 4. Effect of hFcRn binding affinity at neutral pH on antigen sweeping profile in hFcRn-Tgm. (A, B) Effect of FcRn binding affinity at pH 7.0 on antigen sweeping and antibody pharmacokinetics in hFcRn-Tgm steady-state model with hsIL-6R concentration of approximately 20 ng/mL in the presence of human IgG. NPH-IgG1, PH-IgG1, PH-v3, v4, v5 and v6 were intravenously administered as single doses of 1 mg/kg with 1 g/kg of hIgG. Time profiles of total hsIL-6R plasma concentration (A) and antibody plasma concentration (B) are shown. Each data point represents the mean ± s.d. (n = 3–6 each).
doi:10.1371/journal.pone.0063236.g004

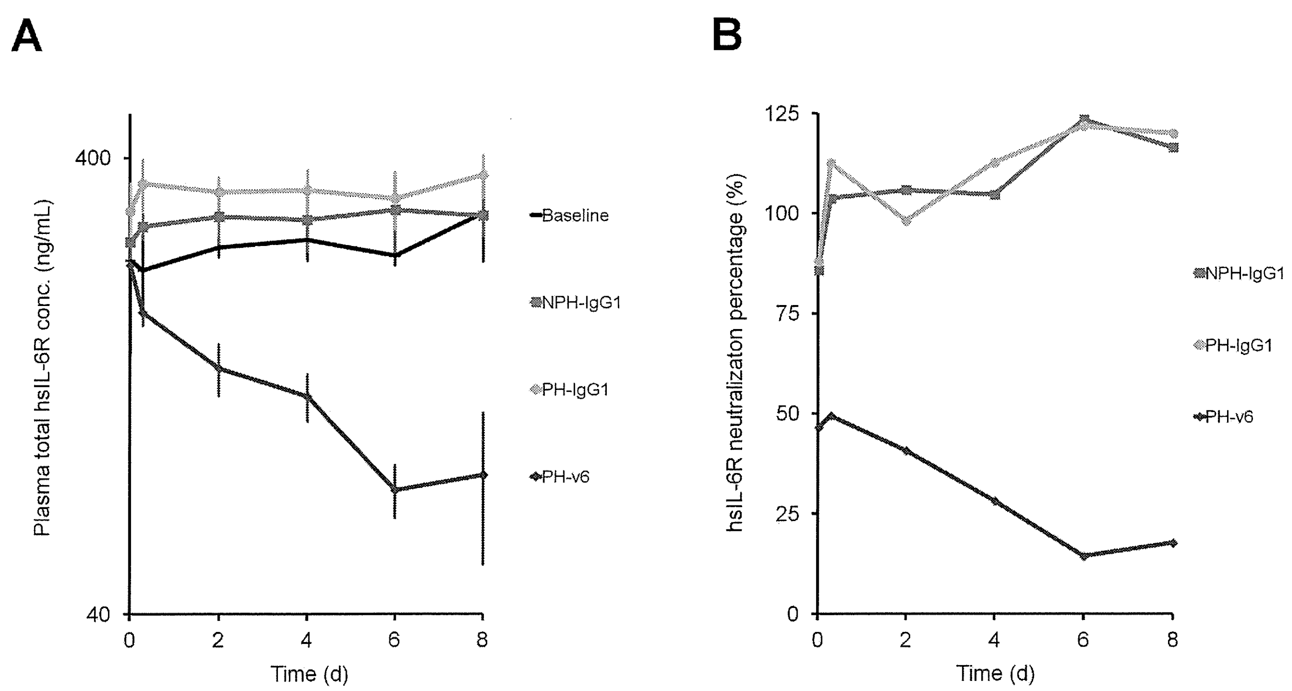

Figure 5. Effect of sweeping antibody on high plasma concentration antigen. Effect of NPH-IgG1, PH-IgG1 and PH-v6 on a hFcRn-Tgm steady-state model with high hsIL-6R concentration of approximately 250 ng/mL in the presence of human IgG. NPH-IgG1, PH-IgG1 and PH-v6 were intravenously administered as multiple doses of 0.01 mg/kg every other day. Molar baseline hsIL-6R concentration (6.6 nM) is 5-fold higher than antibody concentration at 15 min (1.3 nM). Time profiles of total hsIL-6R plasma concentration (A) and free hsIL-6R percentage over control (B) are shown. Each data point represents the mean ± s.d. for total hsIL-6R concentration (n = 3–5 each). Free hsIL-6R percentage over control is determined from the pooled plasma sample of n = 3–5 each.
doi:10.1371/journal.pone.0063236.g005

endocytosis. However, our study demonstrated that antibody with increased FcRn binding affinity at neutral pH without pH-dependent antigen binding (NPH-v2) could not actively eliminate the antigen from plasma because the antigen is also recycled back to plasma by FcRn in the antibody-antigen complex.

Combining a pH-dependent antigen binding with increased FcRn binding at only acidic pH (PH-YTE) attenuated rather than accelerated antigen clearance compared to pH-dependent antigen-binding antibody with wild type IgG1 (PH-IgG1), probably because the improved endosomal recycling efficiency [19] also applied to the antigen that remained bound to the antibody. In addition, non-FcRn binding Fc (PH-NB) could not actively eliminate the antigen from plasma because, similar to PH-IgG1, the uptake of antibody-antigen complex into the cell was marginal.

Antigen sweeping was only achieved by the combination of pH-dependent antigen binding with increased FcRn binding affinity at neutral pH (PH-v2). These studies support the following mechanism of sweeping antibody, mimicking the process of rapid ligand sweeping by endocytic receptors [13–15] (Fig. S2C): (i) increasing binding affinity to FcRn at neutral pH anchors the antibody to the cell surface and provides FcRn-mediated cellular uptake of antibody-antigen complex, (ii) pH-dependent dissociation of antibody-antigen complex enables selective degradation of the antigen, (iii) FcRn-mediated recycling of the free antibody to the cell surface enables another round of the cycle. Because this cycle has a rapid turnover rate and FcRn is broadly expressed in the body, sweeping antibody can effectively eliminate the antigen from plasma.

As our results show, this antigen-sweeping activity can be successfully applied either to antibody which has no *in vitro* hsIL-6R neutralizing activity (PHX-v1) to create *in vivo* inhibition of hsIL-6R/hIL-6-mediated trans-signaling or to convert conventional antibody with *in vitro* activity (NPH-IgG1) into sweeping antibody (PH-v1) to further potentiate the *in vivo* signaling inhibition. This study demonstrated that *in vivo* efficacy of sweeping antibody required no *in vitro* biological activity, indicating that sweeping antibody could antagonize multi-epitope antigen (antigen with multiple functional epitope) or toxic antigen with no functional epitope, which cannot be antagonized with a conventional antibody, by directly eliminating the antigen from plasma. Moreover, this study also demonstrated that conventional antibody with biological activity *in vitro* can be further potentiated *in vivo* by engineering the antibody into sweeping antibody, indicating that engineering conventional antibody into sweeping antibody could be an alternative approach to enhancing the therapeutic efficacy of conventional antibody.

Since sweeping antibody would compete with endogenous IgG to bind to FcRn, it was assumed that endogenous IgG would affect the efficiency of antigen sweeping. A similar phenomenon has been reported for antibody-dependent cellular cytotoxicity mediated by Fc gamma receptor binding, which was significantly inhibited by the presence of endogenous hIgG [34]. As expected, antigen sweeping in hFcRn-Tgm was significantly attenuated in the presence of hIgG when hIgG concentration was maintained at an average of 10 mg/mL (reflecting the clinical situation where endogenous hIgG is approximately 10 mg/mL [20]). This demonstrates that endogenous IgG is an important factor in the efficacy of sweeping antibody when considering clinical applications. It has been reported that IgG with increased FcRn binding at neutral pH (Abdeg) accelerates the clearance of endogenous IgG by blocking FcRn [35]. However, we did not observe accelerated clearance of hIgG in the presence of v4-type sweeping antibody (data not shown). Since reported Abdeg (with FcRn binding affinity of 7.4 nM at pH 7.2) accelerated the clearance of endogenous IgG at a dose of approximately 8 mg/kg, it is expected that v4-type sweeping antibody (with FcRn binding affinity of 120 nM at pH 7.0 significantly lower than Abdeg) would not accelerate the clearance of endogenous IgG at a therapeutically relevant dosage, although a high dosage of v6-type sweeping antibody (with stronger FcRn binding affinity of 35 nM at pH 7.0) may have some effect on the clearance of endogenous IgG.

The effect of hFcRn binding affinity at neutral pH on the antigen sweeping profile and antibody pharmacokinetics was investigated by evaluating Fc variants v3 to v6 in hFcRn-Tgm in the presence of hIgG. The results clearly demonstrate that both antigen sweeping and antibody pharmacokinetics depend on hFcRn binding affinity at neutral pH. By increasing the binding affinity at neutral pH, the extent of antigen sweeping (reflected by minimum total hsIL-6R plasma concentration (Table S2)) was enhanced but the duration of antigen sweeping was shortened and antibody clearance was increased. Compared to conventional antibody (NPH-IgG1), all sweeping antibody exhibited stronger reduction of free antigen plasma concentration, which determines the *in vivo* efficacy as a therapeutic antibody, and the extent and the duration of free antigen reduction depended on hFcRn binding affinity (Fig. S3).

Sweeping antibody with moderate hFcRn binding affinity at neutral pH provides moderate but long-acting antigen sweeping. Specifically, compared to conventional antibody (NPH-IgG1), sweeping antibody with hFcRn binding affinity of 120 nM (PH-v4) maintains a similar antibody plasma concentration and provides long-lasting approximately 50-fold reduction of total antigen plasma concentration. Importantly, this demonstrates that the antigen, not the antibody, is selectively eliminated from the plasma. To systematically understand the therapeutic advantage of this v4-type sweeping antibody, modeling and simulation [30] was conducted based on the experimental result of the hFcRn-Tgm study (Fig. S4A, Table S3). The simulation was conducted to calculate the dosage required to neutralize 95% of hsIL-6R (baseline 250 ng/mL) by once-a-month dosing using conventional, pH-dependent antigen binding, and v4-type sweeping antibodies with different binding affinity to hsIL-6R (Fig. S4B). In the simulation study, the dosage of conventional antibody cannot be lowered below 45 mg/kg even with infinite affinity, whereas sweeping antibody with only 0.1 nM affinity can be effective at 1.4 mg/kg. This demonstrates that v4-type sweeping antibody provides more than 30-fold reduction of dosage over conventional antibody even with infinite affinity, a level which can never be achieved with conventional antibody.

On the other hand, sweeping antibody with hFcRn binding affinity below 80 nM provides short-lasting but extensive reduction of antigen plasma concentration compared to conventional antibody. Specifically, sweeping antibody with hFcRn binding affinity of 35 nM (PH-v6) reduces antigen concentration approximately 1000-fold compared to conventional antibody, while the antibody clearance is increased only 4-fold. To understand the therapeutic advantage of v6-type sweeping antibody, antibodies were tested under conditions in which an excess molar amount of antigen was present in plasma, mimicking the therapeutic situation where antigen is present at a high concentration. This excess amount of antigen, which, as expected, conventional antibody (NPH-IgG1) or pH-dependent binding antibody (PH-IgG1) could not antagonize, was antagonized by sweeping antibody (PH-v6) by reducing the plasma antigen concentration below the baseline. This study demonstrated that sweeping antibody could antagonize high concentration antigen against which conventional or pH-dependent antigen binding antibody, even with infinite affinity, would be completely ineffective.

We believe that sweeping antibody, an engineered monoclonal antibody with novel antigen-sweeping activity, provides potential advantages over conventional antibody that can only bind to the antigen and accumulates the antigen in plasma. First, sweeping antibody could be applied to high concentration antigens or antigens with rapid clearance which conventional antibodies, even with infinite affinity, have previously had difficulty in targeting. Second, by directly eliminating the antigen from plasma, sweeping antibody could be applied to antagonize multi-epitope antigen or toxic antigens without functional epitope, which cannot be simply antagonized by a conventional antibody. These two points suggest that sweeping antibody may expand the target antigen space of therapeutic monoclonal antibody to include target antigens which were previously undruggable by conventional monoclonal antibody. Third, sweeping antibody could provide an alternative approach to affinity maturation against the antigen by reducing the plasma antigen concentration to potentiate the efficacy of conventional antibody [36]. Fourth, sweeping antibody could provide a significant advantage over conventional antibody (even assuming infinite affinity) in dosing by enabling the convenience of subcutaneous and less frequent injections, or in manufacturing by reducing the cost. Since changing the binding affinity to hFcRn generates antibodies with different extent and duration of antigen sweeping, antigen-sweeping profiles can be readily customized. We have applied sweeping antibody technology to various antigens such as IL6, IgA, soluble plexin A1, soluble CD4 and other antigens. We have identified pH-dependent antibodies against each of these antigens and engineered them to bind to FcRn at neutral pH. All of these antibodies demonstrated similar antigen sweeping effect that is shown in this study using hsIL-6R (data not shown). These results suggest that sweeping antibody can be broadly applicable to various antigens.

Supporting Information

Figure S1 Effect of high concentration hIgG on antigen sweeping in hFcRn-Tgm. NPH-IgG1, PH-IgG1 and PH-v2 were intravenously administered as single doses of 1 mg/kg either with or without 1 g/kg of hIgG to hFcRn-Tgm with steady-state hsIL-6R concentration of approximately 20 ng/mL. Time profile of total hsIL-6R plasma concentration is shown. Each data point represents the mean ± s.d. (n = 3 each).
(TIF)

Figure S2 Proposed mode of action of sweeping antibody in comparison with conventional and pH-dependent binding antibody. (A) Conventional antibody bound to soluble antigen is non-specifically taken up by pinocytosis, and binds to FcRn in acidic endosome. Antibody-antigen complex is recycled back to the cell surface and released from FcRn back to plasma. (B) pH-dependent binding antibody (recycling antibody) bound to soluble antigen is non-specifically taken up by pinocytosis, and binds to FcRn in acidic endosome, while antigen is dissociated from the antibody, transferred into lysosome and degraded. Antibody is recycled back to the cell surface by FcRn, released from FcRn back to plasma and binds to another antigen, allowing single antibody to bind to antigen multiple times. (C) Sweeping antibody bound to soluble antigen is rapidly taken up by FcRn-mediated endocytosis. In acidic endosome, antibody binds to FcRn, and antigen is dissociated from the antibody, transferred into lysosome and degraded. Antibody is recycled back to the cell surface and either released from FcRn back to plasma or stays bound to FcRn on the cell surface to bind to another antigen. Rapid FcRn-mediated uptake allows enhanced lysosomal antigen degradation rate.
(TIF)

Figure S3 Antigen sweeping profile of antibodies with different hFcRn binding affinity at neutral pH in hFcRn-Tgm. Effect of FcRn binding affinity at pH 7.0 on antigen sweeping and antibody pharmacokinetics in hFcRn-Tgm with steady-state hsIL-6R concentration of approximately 20 ng/mL in the presence of human IgG. NPH-IgG1, PH-IgG1, PH-v3, v4, v5 and v6 were intravenously administered as single doses of 1 mg/kg with 1 g/kg of hIgG. Theoretical free hsIL-6R plasma concentration was calculated from plasma antibody concentration, total hsIL-6R concentration and binding affinity to hsIL-6R. Time profile of theoretical free hsIL-6R plasma concentration is shown.
(TIF)

Figure S4 Modeling and simulation of sweeping antibody. (A) Antibody-antigen dynamic model of sweeping antibody. Antibody is injected intravenously to the central compartment and distributed to the peripheral compartment. Antibody binds to the antigen in the central compartment. Antibody, antigen and antibody-antigen complex are eliminated from the central compartment. Effect of pH-dependent binding and increased binding affinity to FcRn is reflected in the elimination rate of antibody-antigen complex. Parameters used in this model are k_{synthe} (rate constant of antigen synthesis), $C_{antigen,baseline}$ (baseline concentration of antigen), $k_{el,antigen}$ (elimination rate constant of antigen), $Vd1_{antigen}$ (volume of distribution of antigen), $k_{12,antigen}$ (transfer rate constant of antigen from central to peripheral compartment), $k_{21,antigen}$ (transfer rate constant of antigen from peripheral to central compartment), $k_{el,mab}$ (elimination rate constant of antibody), $Vd1_{mab}$ (volume of distribution of antibody), $k_{12,mab}$ (transfer rate constant of antibody from central to peripheral compartment), $k_{21,mab}$ (transfer rate constant of antibody from peripheral to central compartment) and $k_{el,complex}$ (elimination rate constant of antigen in complex with antibody). Note that antibody in complex with antigen is eliminated at the rate of $k_{el,mab}$. (B) Simulation of required dosage to neutralize antigen (baseline concentration 250 ng/mL) by 95% at trough with dosing once a month using conventional antibody (non-pH dependent binding IgG1 antibody), pH-dependent binding IgG1 antibody and v4-type sweeping antibody with different binding affinity to the antigen. Relationship between the antigen binding affinity (K_D) and the antibody dosage required to achieve once monthly dosing is shown.
(TIF)

Table S1 Binding affinity of the anti-IL-6R IgG1 antibodies.
(TIF)

Table S2 Antibody clearance and minimum or maximum total hsIL-6R plasma concentration for tested antibodies.
(TIF)

Table S3 Fitted pharmacokinetic parameters in antibody-antigen dynamic model.
(TIF)

Acknowledgements

We thank colleagues in Chugai Research Institute for Medical Science, Inc, and Chugai Pharmaceutical Co. Ltd., Y. Kawase and H. Tateishi for breeding hFcRn-Tgm; M. Hirabayashi, M. Kinoshita, Yuichiro Ochiai, K. Koguchi, H. Sano, Yuichi Ochiai, T. Sakamoto, M. Kawaharada, T. Yokoyama and T. Nishimura for carrying out *in vivo* studies; M. Fujii, S.

Masujima and A. Takara for antibody generation; and W. Hatakeyama, M. Saito and Y. Okura for carrying out SPR and *in vitro* analysis.

Author Contributions

Provided direction and guidance: HT K. Hattori. Conceived and designed the experiments: TI. Performed the experiments: AM K. Haraya TT YI KN YH SI. Analyzed the data: K. Haraya TT YI FM. Contributed reagents/materials/analysis tools: NH ST TW. Wrote the paper: TI.

References

1. Chan AC, Carter PJ (2010) Therapeutic antibodies for autoimmunity and inflammation. Nature Rev Immunol 10: 301–316.
2. Weiner LM, Surana R, Wang S (2010) Monoclonal antibodies, versatile platforms for cancer immunotherapy. Nature Rev Immunol 10: 317–327.
3. Davda JP, Hansen RJ (2010) Properties of a general PK/PD model of antibody-ligand interactions for therapeutic antibodies that bind to soluble endogenous targets. MAbs: 2, 576–588.
4. Haringman JJ, Gerlag DM, Smeets TJ, Baeten D, van den Bosch F, et al. (2006) A randomized controlled trial with an anti-CCL2 (anti-monocyte chemotactic protein 1) monoclonal antibody in patients with rheumatoid arthritis. ARTHRITIS and RHEUMATISM 54: 2387–2392.
5. Xiao JJ, Krzyzanski W, Wang YM, Li H, Rose MJ, et al. (2010) Pharmacokinetics of anti-hepcidin monoclonal antibody Ab 12B9m and hepcidin in cynomolgus monkeys. AAPS J 12: 646–657.
6. Martin PL, Cornacoff J, Prabhakar U, Lohr T, Treacy G, et al. (2005) Preclinical Safety and Immune-Modulating Effects of Therapeutic Monoclonal Antibodies to Interleukin-6 and Tumor Necrosis Factor-alpha in Cynomolgus Macaques. J Immunotoxicol 3: 131–139.
7. Byrd JC, O'Brien S, Flinn IW, Kipps TJ, Weiss M, et al. (2007) Phase 1 study of lumiliximab with detailed pharmacokinetic and pharmacodynamic measurements in patients with relapsed or refractory chronic lymphocytic leukemia. Clin Cancer Res 13: 4448–4455.
8. Jayson GC, Mulatero C, Ranson M, Zweit J, Jackson A, et al. (2005) Phase I investigation of recombinant anti-human vascular endothelial growth factor antibody in patients with advanced cancer. Eur J Cancer 41: 555–563.
9. Finkelman FD, Madden KB, Morris SC, Holmes JM, Boiani N, et al. (1993) Anti-cytokine antibodies as carrier proteins. Prolongation of in vivo effects of exogenous cytokines by injection of cytokine-anti-cytokine antibody complexes. J Immunol 151: 1235–1244.
10. Davis CB, Tobia LP, Kwok DC, Oishi CM, Kheterpal N, et al. (1999) Accumulation of Antibody-Target Complexes and the Pharmacodynamics of Clotting after Single Intravenous Administration of Humanized Anti-Factor IX Monoclonal Antibody to Rats. Drug Delivery 6: 171–179.
11. Zareba KM (2007) Eculizumab, A novel therapy for paroxysmal nocturnal hemoglobinuria. Drugs Today (Barc) 43: 539–46.
12. Rathanaswami P, Roalstad S, Roskos L, Su QJ, Lackie S, et al. (2005) Demonstration of an in vivo generated sub-picomolar affinity fully human monoclonal antibody to interleukin-8. Biochem Biophys Res Commun 334: 1004–1013.
13. Feinberg H, Torgersen D, Drickamer K, Weis WI (2000) Mechanism of pH-dependent N-acetylgalactosamine binding by a functional mimic of the hepatocyte asialoglycoprotein receptor. J Biol Chem 275: 35176–35184.
14. Yamamoto T, Chen HC, Guigard E, Kay CM, Ryan RO (2008) Molecular studies of pH-dependent ligand interactions with the low-density lipoprotein receptor. Biochemistry 47: 11647–11652.
15. French AR, Tadaki DK, Niyogi SK, Lauffenburger DA (1995) Intracellular trafficking of epidermal growth factor family ligands is directly influenced by the pH sensitivity of the receptor/ligand interaction. J Biol Chem 270: 4334–4340.
16. Igawa T, Ishii S, Tachibana T, Maeda A, Higuchi Y, et al. (2010) Antibody recycling by engineered pH-dependent antigen binding improves the duration of antigen neutralization. Nat Biotechnol 28: 1203–1207.
17. Jostock T, Müllberg J, Ozbek S, Atreya R, Blinn G, et al. (2001) Soluble gp130 is the natural inhibitor of soluble interleukin-6 receptor transsignaling responses. Eur J Biochem 268: 160–167.
18. Dall'Acqua WF, Woods RM, Ward ES, Palaszynski SR, Patel NK, et al. (2002) Increasing the affinity of a human IgG1 for the neonatal Fc receptor:biological consequences. J Immunol 169: 5171–5180.
19. Dall'Acqua WF, Kiener PA, Wu H (2006) Properties of human IgG1s engineered for enhanced binding to the neonatal Fc receptor (FcRn). J Biol Chem 281: 23514–23524.
20. Petkova SB, Akilesh S, Sproule TJ, Christianson GJ, Al Khabbaz H, et al. (2006) Enhanced half-life of genetically engineered human IgG1 antibodies in a humanized FcRn mouse model, potential application in humorally mediated autoimmune disease. Int Immunol 18: 1759–1769.
21. Yeung YA, Leabman MK, Marvin JS, Qiu J, Adams CW, et al. (2009) Engineering human IgG1 affinity to human neonatal Fc receptor, impact of affinity improvement on pharmacokinetics in primates. J Immunol 182: 7663–7671.
22. Datta-Mannan A, Witcher DR, Tang Y, Watkins J, Wroblewski VJ (2007) Monoclonal antibody clearance. Impact of modulating the interaction of IgG with the neonatal Fc receptor. J Biol Chem 282: 1709–1717.
23. Deng R, Loyet KM, Lien S, Iyer S, DeForge LE, et al. (2010) Pharmacokinetics of humanized monoclonal anti-tumor necrosis factor-{alpha} antibody and its neonatal Fc receptor variants in mice and cynomolgus monkeys. Drug Metab Dispos 38: 600–605.
24. Dall'Acqua WF, Kiener PA, Wu H (2006) Properties of human IgG1s engineered for enhanced binding to the neonatal Fc receptor (FcRn). J Biol Chem. 281, 23514–23524.
25. Hinton PR, Xiong JM, Johlfs MG, Tang MT, Keller S, et al. (2006) An engineered human IgG1 antibody with longer serum half-life. J Immunol 176: 346–356.
26. Zalevsky J, Chamberlain AK, Horton HM, Karki S, Leung IW, et al. (2010) Enhanced antibody half-life improves in vivo activity. Nat Biotechnol 28: 157–159.
27. Roopenian DC, Christianson GJ, Sproule TJ (2010) Human FcRn transgenic mice for pharmacokinetic evaluation of therapeutic antibodies. Methods Mol Biol 602: 93–104.
28. Okazaki M, Yamada Y, Nishimoto N, Yoshizaki K, Mihara M (2002) Characterization of anti-mouse interleukin-6 receptor antibody. Immunol Lett 84: 231–240.
29. Rashid A, Auchincloss H Jr, Sharon J (1992) Comparison of GK1.5 and chimeric rat/mouse GK1.5 anti-CD4 antibodies for prolongation of skin allograft survival and suppression of alloantibody production in mice. J Immunol 148: 1382–1388.
30. Betts AM, Clark TH, Yang J, Treadway JL, Li M, et al. (2010) The application of target information and preclinical pharmacokinetic/pharmacodynamic modeling in predicting clinical doses of a Dickkopf-1 antibody for osteoporosis. J Pharmacol Exp Ther 333: 2–13.
31. Ozbek S, Peters M, Breuhahn K, Mann A, Blessing M, et al. (2001) The designer cytokine hyper-IL-6 mediates growth inhibition and GM-CSF-dependent rejection of B16 melanoma cells. Oncogene 20: 972–979.
32. Deng R, Meng YG, Hoyte K, Lutman J, Lu Y, et al. (2012) Subcutaneous bioavailability of therapeutic antibodies as a function of FcRn binding affinity in mice. MAbs 4: 101–109.
33. Ober RJ, Radu CG, Ghetie V, Ward ES (2001) Differences in promiscuity for antibody-FcRn interactions across species, implications for therapeutic antibodies. Int Immunol 13: 1551–1559.
34. Preithner S, Elm S, Lippold S, Locher M, Wolf A, et al. (2006) High concentrations of therapeutic IgG1 antibodies are needed to compensate for inhibition of antibody-dependent cellular cytotoxicity by excess endogenous immunoglobulin G. Mol Immunol 43: 1183–1193.
35. Vaccaro C, Zhou J, Ober RJ, Ward ES (2005) Engineering the Fc region of immunoglobulin G to modulate in vivo antibody levels. Nat Biotechnol 23: 1283–1288.
36. Finch DK, Sleeman MA, Moisan J, Ferraro F, Botterell S, et al. (2011) Whole-molecule antibody engineering: generation of a high-affinity anti-IL-6 antibody with extended pharmacokinetics. J Mol Biol 411: 791–807.

Identification and Multidimensional Optimization of an Asymmetric Bispecific IgG Antibody Mimicking the Function of Factor VIII Cofactor Activity

Zenjiro Sampei, Tomoyuki Igawa*, Tetsuhiro Soeda, Yukiko Okuyama-Nishida, Chifumi Moriyama, Tetsuya Wakabayashi, Eriko Tanaka, Atsushi Muto, Tetsuo Kojima, Takehisa Kitazawa, Kazutaka Yoshihashi, Aya Harada, Miho Funaki, Kenta Haraya, Tatsuhiko Tachibana, Sachiyo Suzuki, Keiko Esaki, Yoshiaki Nabuchi, Kunihiro Hattori

Research Division, Chugai Pharmaceutical Co., Ltd., Gotemba, Shizuoka, Japan

Abstract

In hemophilia A, routine prophylaxis with exogenous factor VIII (FVIII) requires frequent intravenous injections and can lead to the development of anti-FVIII alloantibodies (FVIII inhibitors). To overcome these drawbacks, we screened asymmetric bispecific IgG antibodies to factor IXa (FIXa) and factor X (FX), mimicking the FVIII cofactor function. Since the therapeutic potential of the lead bispecific antibody was marginal, FVIII-mimetic activity was improved by modifying its binding properties to FIXa and FX, and the pharmacokinetics was improved by engineering the charge properties of the variable region. Difficulties in manufacturing the bispecific antibody were overcome by identifying a common light chain for the anti-FIXa and anti-FX heavy chains through framework/complementarity determining region shuffling, and by pI engineering of the two heavy chains to facilitate ion exchange chromatographic purification of the bispecific antibody from the mixture of byproducts. Engineering to overcome low solubility and deamidation was also performed. The multidimensionally optimized bispecific antibody hBS910 exhibited potent FVIII-mimetic activity in human FVIII-deficient plasma, and had a half-life of 3 weeks and high subcutaneous bioavailability in cynomolgus monkeys. Importantly, the activity of hBS910 was not affected by FVIII inhibitors, while anti-hBS910 antibodies did not inhibit FVIII activity, allowing the use of hBS910 without considering the development or presence of FVIII inhibitors. Furthermore, hBS910 could be purified on a large manufacturing scale and formulated into a subcutaneously injectable liquid formulation for clinical use. These features of hBS910 enable routine prophylaxis by subcutaneous delivery at a long dosing interval without considering the development or presence of FVIII inhibitors. We expect that hBS910 (investigational drug name: ACE910) will provide significant benefit for severe hemophilia A patients.

Citation: Sampei Z, Igawa T, Soeda T, Okuyama-Nishida Y, Moriyama C, et al. (2013) Identification and Multidimensional Optimization of an Asymmetric Bispecific IgG Antibody Mimicking the Function of Factor VIII Cofactor Activity. PLoS ONE 8(2): e57479. doi:10.1371/journal.pone.0057479

Editor: Peter J. Lenting, Institut National de la Santé et de la Recherche Médicale, France

Received October 24, 2012; **Accepted** January 21, 2013; **Published** February 28, 2013

Funding: Chugai Pharmaceutical Co., Ltd. supported and funded the research described in this report. The funders authorized our decision to publish, but had no role in study design, data collection and analysis, or preparation of the manuscript.

Competing Interests: All authors are employees of Chugai Pharmaceutical Co., Ltd. which is conducting the clinical study of hBS910 (ACE910). TS, T. Kojima and KH are inventors of the patents and patent applications which claim FVIII-mimetic bispecific antibodies to FIXa and FX. ZS, TI, TS, YON, CM, AM, T. Kojima, T. Kitazawa and KY are inventors of the patent application which claims hBS910, the investigational drug. These do not alter the authors' adherence to all the PLOS ONE policies on sharing data and materials.

* E-mail: igawatmy@chugai-pharm.co.jp

Introduction

Hemophilia A is caused by an X-linked inherited dysfunction of coagulation factor VIII (FVIII). Patients with severe hemophilia A, who have plasma FVIII levels of less than 1% of normal, typically experience bleeding events several times a month [1]. Routine supplementation with exogenous human FVIII to maintain FVIII levels at 1% of normal or above is effective for reducing joint bleeding events and improving joint status and health-related quality of life in hemophilia A patients [2]. However, there are two major drawbacks to this prophylactic usage of exogenous FVIII. The first drawback is the necessity of frequent intravenous administration: three intravenous injections weekly of FVIII are necessary because of its low subcutaneous bioavailability and its short plasma half-life [3,4,5]. The second drawback is the development of inhibitory anti-FVIII alloantibodies, known as "inhibitors" [6]. Once FVIII inhibitors have developed, routine supplementation with exogenous FVIII will be no longer effective and the usage of exogenous FVIII for treating on-going bleeds is restricted. In such cases, alternative agents, such as activated factor VII and activated prothrombin complex concentrate, which are more expensive and have less stable hemostatic effects, need to be used to control bleeding [7,8]. Therefore, a new agent that resolves these drawbacks of exogenous FVIII is awaited in the field of the bleeding prophylaxis of severe hemophilia A.

Monoclonal antibodies have become an important therapeutic option in numerous diseases and are expected to play a greater role in the future of disease treatment [9,10]. Various monoclonal antibodies have been generated [11]; these not only include those with antagonistic activity but also those with agonistic activity [12], catalytic activity [13], and allosteric activity [14]. Antibody engineering technologies to generate bispecific antibodies have been extensively studied due to the huge potential of these antibodies for therapeutic applications [15]. Bispecific antibodies can be applied to simultaneously target two disease related antigens, retarget effector cells against the target cell [16], and co-ligate two different antigens on the same cell [17].

FVIII is cleaved by thrombin or factor Xa (FXa), and the resultant factor VIIIa (FVIIIa) presents a heterotrimeric structure consisting of the A1 subunit, the A2 subunit, and the light chain [18]. Simultaneous binding of FVIIIa to FIXa and FX by the light chain and the A2 subunit, and by the A1 subunit, respectively, contributes to FVIII cofactor activity which places FIXa and FX into proximity, and also allosterically enhances the catalytic rate constant of FIXa [19,20,21,22,23] (Fig. 1A).

Considering this function of FVIII and the versatilities of antibodies, we hypothesized that a bispecific antibody recognizing FIXa with one arm and FX with the other arm could mimic the FVIII cofactor activity by placing FIXa and FX in spatially appropriate positions, and by allosterically enhancing the catalytic activity of FIXa (Fig. 1B) [23]. We have recently reported a recombinant humanized bispecific antibody to FIXa and FX, termed hBS23, which exerted coagulation activity in FVIII-deficient plasma, even in the presence of FVIII inhibitors, and showed *in vivo* hemostatic activity in a cynomolgus monkey model of acquired hemophilia A, and had high subcutaneous bio-availability and a 2-week half-life in cynomolgus monkey [23]. Although the pharmacological concept of FVIII-mimetic bispecific antibody was clearly demonstrated in this report, the detail of this anti-FIXa/FX asymmetric bispecific IgG antibody identification was not described, and moreover, it required further optimization in several ways before the clinical use of such an agent in humans.

For therapeutic development, optimization of the bispecific antibody by molecular engineering to enable large-scale manufacturing of the bispecific antibody at clinical grade would be required. Although a variety of molecular formats for bispecific antibodies have been studied, including single-chain diabody, tandem scFv, IgG-scFv, DVD-Ig, CrossMab, and dual-binding Fab [24], we selected an asymmetric bispecific IgG format because it is the only format that can recognize FIXa and FX with each arm and has a long half-life and a native IgG structure. However, recombinant production of this format is challenging in comparison to the other formats because it consists of two different heavy chains and two different light chains which would result in the secretion of a mixture of ten different combinations of heavy and light chains [25]. Purification of one desired bispecific antibody from a mixture including nine miss-paired byproducts is nearly impossible. Engineering technologies to resolve such a difficulty have been previously reported. First, identification of a common light chain by phage display as the partner of the two heavy chains can reduce the number of heavy and light combinations to three: one heterodimeric bispecific antibody and two homodimeric

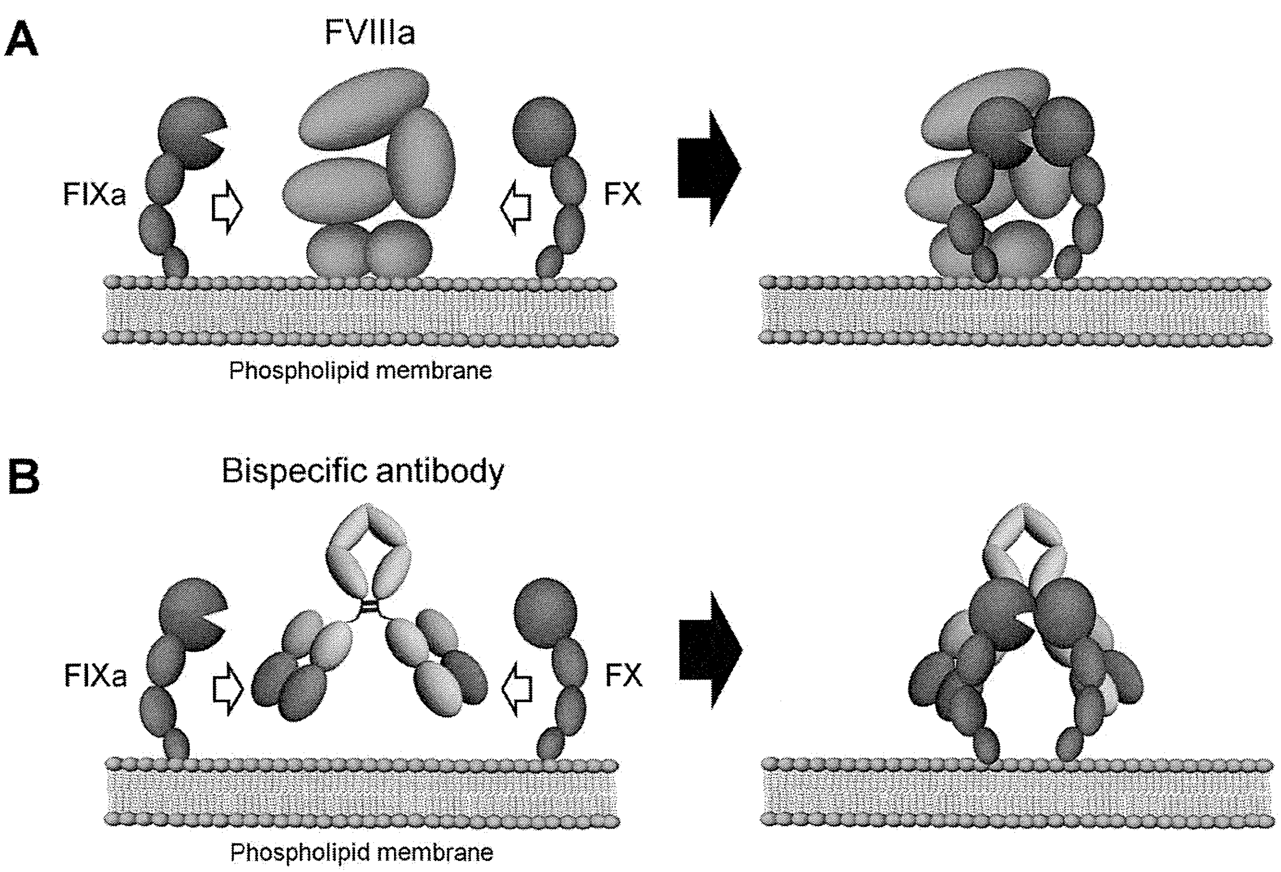

Figure 1. Schematic illustrations of cofactor actions of FVIIIa and a bispecific antibody promoting the interaction between FIXa and FX. (A) FVIIIa forms a complex with FIXa and supports the interaction between FIXa and FX through its binding ability to both factors on the phospholipid membrane. (B) A bispecific antibody binding to FIXa and FX would promote the interaction between FIXa and FX and exert FVIII-mimetic activity on the phospholipid membrane.
doi:10.1371/journal.pone.0057479.g001

monospecific antibodies [26]. However, selection of a common light chain with potent FVIII-mimetic activity based on the binding affinity by phage display was not feasible for our bispecific antibody, because higher binding affinities was considered not to lead to higher activity. To date, alternative approach to obtain common light chain has not been reported. Second, engineering the C_H3 domain to facilitate Fc heterodimerization can minimize the amount of homodimeric byproducts [25,26]. Nevertheless, the efficiency of heterodimerization is not complete; therefore, a small amount of homodimeric byproduct is formed, which needs to be removed in the downstream purification process. However, because the biophysical properties of the homodimeric byproducts are often similar to those of the target bispecific antibody, purifying the target bispecific antibody on a large scale for clinical applications is still challenging. To date, technologies to address this issue have not been reported. Therefore, improving the manufacturability of this type of FVIII-mimetic antibody by molecular engineering is required for therapeutic application.

Moreover, for maximizing the therapeutic potential of FVIII-mimetic bispecific antibody, optimization to increase the FVIII-mimetic activity of the bispecific antibody, prolong the half-life, improve the physicochemical properties of the antibody and reduce the immunogenicity of the humanized antibody would be required. This would enable more effective and long-term prophylaxis with stronger hemostatic effect for hemophilia A patients by a subcutaneous formulation with a longer dosing interval.

In this paper, we report molecular identification and multidimensional optimization of a FVIII-mimetic bispecific antibody which can be used for clinical application. At the start of this study, we examined bispecific combinations of large number of monoclonal anti-FIXa and anti-FX antibodies, and identified the lead anti-FIXa/FX bispecific IgG antibody having FVIII-mimetic activity. Then, this lead bispecific antibody was subjected to multidimensional optimization processes [27] to improve both its therapeutic potential and manufacturability. We successfully generated a humanized bispecific IgG antibody having sufficient FVIII-mimetic activity for prophylactic use even in the presence of FVIII inhibitors, high subcutaneous bioavailability with an approximately 3-week plasma half-life in cynomolgus monkeys, and minimal immunogenicity risk. In addition, molecular engineering enabled purification on a large manufacturing scale and formulation into a liquid formulation of 150 mg/mL for subcutaneous delivery. We expect that this anti-FIXa/FX bispecific antibody mimicking FVIII cofactor activity will provide significant benefit for managing bleeding events in severe hemophilia A patients.

Results

Research Flow of Identification and Multidimensional Optimization of Lead FVIII-mimetic anti-FIXa/FX Bispecific Antibody

Figure 2 shows the flow of the screening process to identify the lead bispecific antibody with a common light chain (BS15). BS15 was generated by combinatorial screening of bispecific antibodies composed of anti-FIXa and anti-FX antibodies derived from immunization, followed by screening of common light chains and then framework/complementarity determining region (FR/CDR) shuffling.

Figure 3 represents the multidimensional optimization flow to generate the bispecific antibody with the most appropriate properties for clinical application (hBS910) from the lead bispecific antibody (BS15). BS15 was firstly humanized to generate hBS1, followed by engineering to improve FVIII-mimetic activity (hBS106), improve pharmacokinetics (hBS128 and hBS228), enable purification of target bispecific antibody (hBS366 and hBS376), improve solubility (hBS560), remove deamidation site (hBS660), and reduce immunogenicity risk (deimmunization) to generate a multidimensionally optimized bispecific antibody (hBS910). Through this multidimensional optimization process, the numbers of variable region variants that we have generated for anti-FIXa heavy chain, anti-FX heavy chain and common light chain were approximately 500, 300 and 400, respectively, and the number of bispecific IgG antibodies that we have prepared and evaluated is approximately 2,400. Supplementary table S1 represents the number of mutations which were introduced into hBS1 to generate bispecific antibodies described in this report.

Identification of Lead Anti-FIXa/FX Bispecific Antibody with FVIII-mimetic Activity

Approximately 200 monoclonal antibodies against FIXa or FX were obtained from animals immunized with either human FIXa or FX. Approximately 40,000 bispecific IgG antibodies that comprised different combinations of anti-FIXa and anti-FX antibodies in each arm were expressed. Although the expression product of two different heavy chain and two different light chain genes consists of a mixture of ten different species with different heavy and light chain combinations, including the one desired bispecific antibody and the nine miss-paired antibodies (miss-paired antibody includes two homodimeric antibodies with a correct heavy and light chain pair), Fc heterodimerization mutations would theoretically enable expression of an antibody mixture containing at least approximately 20% of the target bispecific antibody (see methods for detail) [25]. A total number of 94 bispecific antibodies, or combinations of anti-FIXa heavy chain and anti-FX heavy chain, which had FVIII-mimetic activity were successfully identified by an enzymatic assay. Heavy chain combinations were selected from the point of high FVIII-mimetic activity, not from the point of the similarity of the cognate light chain.

Next, in order to identify a common light chain for the different heavy chains to FIXa and FX, the selected heavy chain combinations were expressed with either one of cognate light chains. Out of 188 light chain commonized bispecific antibodies, the most potent one, termed c1, which consisted of rat anti-FIXa V_H and mouse anti-FX V_H chimerized with human IgG_4 and rat anti-FIXa V_L chimerized with human κ (c1L), was selected for the next step.

Finally, in order to design a more potent common light chain, we performed FR/CDR shuffling. Since the cognate light chain for the selected anti-FX V_H (c2L) was not effective as a common light chain at all (data not shown), we tried to seek another effective common light chain with a high homology to c2L. From our antibody source, we identified a light chain (c3L) whose CDR sequence had >85% homology to that of c2L, and found out that it was effective as a common light chain for the selected two heavy chains. Therefore, we decided to use c3L for FR/CDR shuffling, too. Then, CDRs of c1L, c2L and c3L were shuffled among each other and grafted onto the FRs of c1L and c3L to generate twenty four light chain variants (supplementary Fig. S2A). Twenty four light chain variants were expressed with the two heavy chains, and the most potent common light chain, BS15L, a mouse–rat hybrid V_L chimerized with human κ, was identified (supplementary Fig. S2B). Thus, the light chain communized bispecific antibody with BS15L was selected as the lead chimeric bispecific IgG antibody (termed BS15).

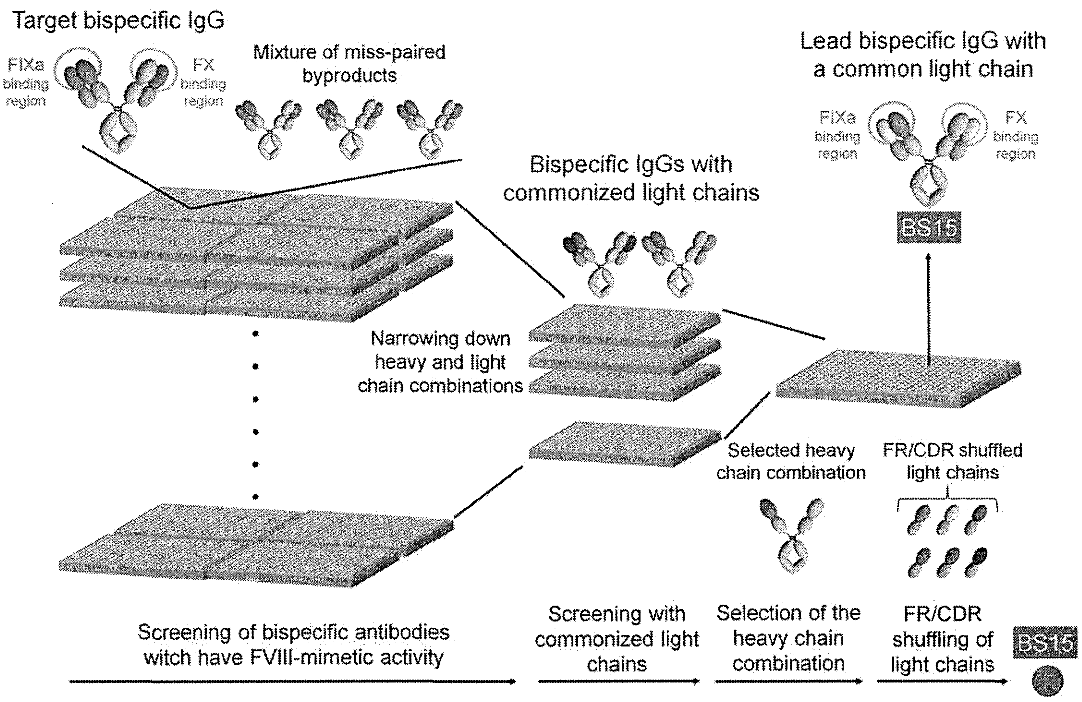

Figure 2. Flow of process to identify the lead bispecific antibody (BS15). BS15 was identified by combinatorial screening of bispecific antibodies, followed by screening of common light chains and then FR/CDR shuffling.
doi:10.1371/journal.pone.0057479.g002

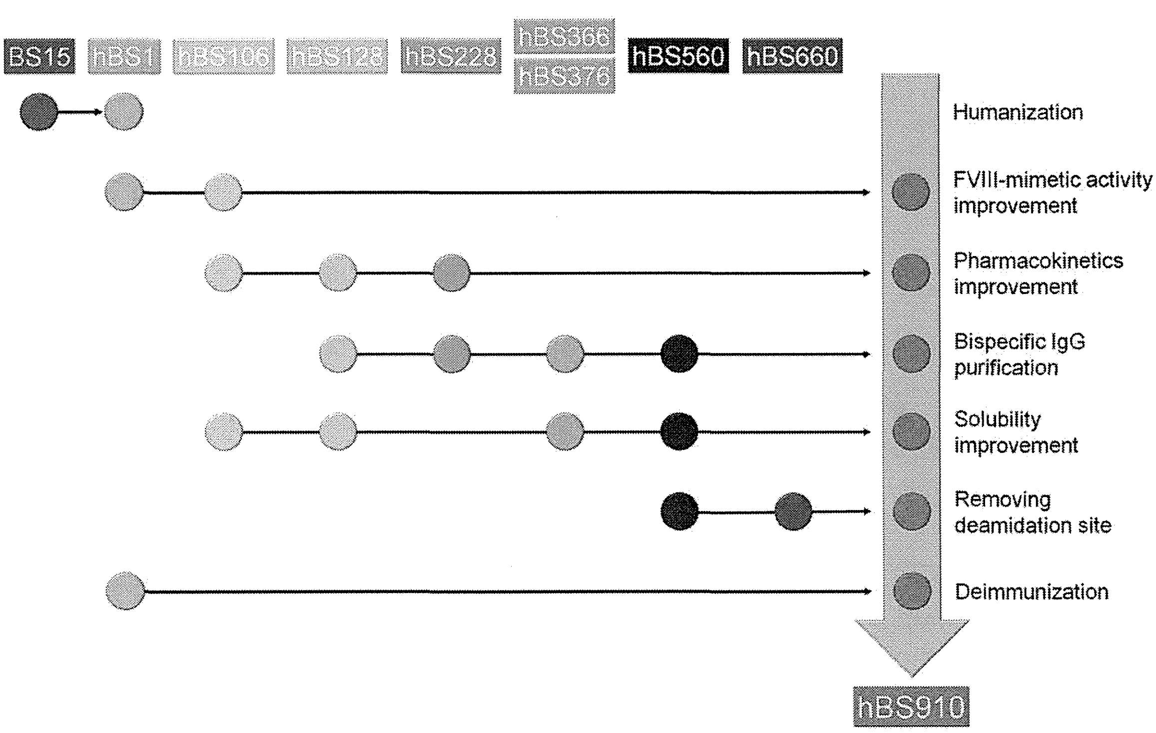

Figure 3. Multidimensional optimization flow to generate the bispecific antibody with most appropriate properties (hBS910). hBS910 was generated through multidimensional optimization with various antibody engineering technologies.
doi:10.1371/journal.pone.0057479.g003